ORIGINAL ARTICLE

Discovery of 4-cyclopropyl-3-(2-((1-cyclopropyl-1*H*-pyrazol-4-yl) amino) quinazolin-6-yl)-*N*-(3-(trifluoromethyl) phenyl) benzamides as potent discoidin domain receptor inhibitors for the treatment of idiopathic pulmonary fibrosis

Qi Wang[a,d,†], Bixi Tang[c,d,f,†], Dandan Sun[g,†], Ying Dong[c,d], Yinchun Ji[b], Huanyu Shi[a,d], Liwei Zhou[a,e], Yueyue Yang[a,d], Menglan Luo[a,i], Qian Tan[c], Lin Chen[a], Yue Dong[h], Cong Li[c], Rongrong Xie[c], Yi Zang[c,d,j], Jingkang Shen[a], Bing Xiong[a,d,*], Jia Li[c,d,g,j,*], Danqi Chen[a,*]

[a]Department of Medicinal Chemistry, Shanghai Institute of Materia Medica, Chinese Academy of Sciences, Shanghai 201203, China
[b]Division of Anti-tumor Pharmacology, State Key Laboratory of Drug Research, Shanghai Institute of Materia Medica, Chinese Academy of Sciences, Shanghai 201203, China
[c]State Key Laboratory of Drug Research, Shanghai Institute of Materia Medica, Chinese Academy of Sciences, Shanghai 201203, China
[d]University of Chinese Academy of Sciences, Beijing 100049, China
[e]Center for Supramolecular Chemistry and Catalysis and Department of Chemistry, College of Sciences, Shanghai University, Shanghai 200444, China
[f]Department of Pharmacology, School of Pharmacy, Fudan University, Shanghai 201203, China
[g]School of Chinese Materia Medica, Nanjing University of Chinese Medicine, Nanjing 210023, China
[h]Department of Pulmonary and Critical Care Medicine, Shanghai Fifth People's Hospital, Fudan University, Shanghai 200240, China
[i]Department of Chemistry, College of Sciences, Shanghai University, Shanghai 200444, China
[j]School of Pharmaceutical Science and Technology, Hangzhou Institute for Advanced Study, UCAS, Hangzhou 310024, China

*Corresponding authors. Tel: +86 21 50806600 5412, fax: +86 21 50807088.

E-mail addresses: bxiong@simm.ac.cn (Bing Xiong), jli@simm.ac.cn (Jia Li),dqchen@simm.ac.cn (Danqi Chen).

†These authors made equal contributions to this work.

Abstract Idiopathic pulmonary fibrosis (IPF) is a chronic fatal lung disease with a median survival time of 3−5 years. Inaccurate diagnosis, limited clinical therapy and high mortality together indicate that the development of effective therapeutics for IPF is an urgent need. In recent years, it was reported that DDRs are potential targets in anti-fibrosis treatment. Based on previous work we carried out further structure modifications and led to a more selective inhibitor **47** by averting some fibrosis-unrelated kinases, such as RET, AXL and ALK. Extensive profiling of compound **47** has demonstrated that it has potent DDR1/2 inhibitory activities, low toxicity, good pharmacokinetic properties and reliable *in vivo* anti-fibrosis efficacy. Therefore, we confirmed that discoidin domain receptors are promising drug targets for IPF, and compound **47** would be a promising candidate for further drug development.

1. Introduction

Interstitial fibrosis is the predominant phenotype in the family of interstitial lung diseases which is not due to infection or cancer[1]. The most common idiopathic interstitial pneumonia is idiopathic pulmonary fibrosis (IPF), a chronic, progressive, fibrotic interstitial lung disease associated with poor survival. Currently, individuals with IPF have similar life expectancy to patients with non-small cell lung cancer, with an estimated median survival about 50% at 3 years and 20% at 5 years after diagnosis[2].

The dynamically altered extracellular matrix (ECM) microenvironment acts as a positive feedback stimulator for lung fibroblast behaviors, reinforces the progression of lung fibrosis. Collagens are the major components of ECM. The vertebrates have a variety of transmembrane receptors that recognize collagens as their ligands, which mainly consists of the integrin family and discoidin domain receptors[3].

Discoidin domain receptors (DDR1 and DDR2) not only belong to the ECM receptors, but also are the members of the receptor tyrosine kinases (RTK)[4,5]. They show distinct signal transduction capability, which initiates from collagens in ECM, and can remarkably delay the signal and sustain long-term activation. This special mechanism endows them to execute particular biological functions in the induction of fibrosis and angiogenesis in lung. At the molecular level, DDR1 is primarily activated by collagens I–IV and VIII, while DDR2 mainly responds to collagen type I and, to a lesser extent, collagen II, III and V. It should be noted that DDR2 does not interact with collagen IV that expresses highly in normal cells[6−8]. In recent years, the biological function of DDR1/2 in the pulmonary fibrosis was gradually revealed. DDR1 deletion has been reported to alleviate bleomycin (BLM)-induced lung inflammation and pulmonary fibrosis by blocking P38 mitogenactivated protein kinase (P38 MAPK) activation[23]. Although DDR2 scarcely expressed in normal lung tissue, the expression of mRNA and protein of DDR2 was dramatically increased in patients with interstitial lung diseases, especially IPF[9,10]. Other studies disclosed that expression of DDR1 could be induced when DDR2 was activated in primary human lung fibroblasts[12]. *In vitro* cellular studies also showed that DDR2 could synergize the actions of both transforming growth factor (TGF)-*β* and fibrillar collagens to stimulate lung fibroblasts to undergo myofibroblastic changes and vascular endothelial growth factor (VEGF) expression[11].

Up to now, several DDR inhibitors had been reported (Fig. 1)[13]. Murray et al.[14] disclosed compound **1** as a low nanomolar DDR1/2, orally bioavailable inhibitor. Jeffries et al.[15] reported the discovery of a potent dual DDR1/2 inhibitor **2** (VU6015929) which potently blocked collagen-induced DDR1 activation and collagen-IV production, suggesting its application for antifibrotic therapy. The development of selective inhibitors was focused on DDR1. Compound **3** was reported by Gao et al.[16] with DDR1 IC$_{50}$ value of 6.8 nmol/L and DDR2 101.4 nmol/L. And it was also significantly less potent to the other 455 kinases tested. Compound **4** was reported by Wang et al.[17], which suppressed DDR1 kinase activity with an IC$_{50}$ value of 9.4 nmol/L and DDR2 188 nmol/L. This compound demonstrated a promising oral therapeutic effect in a bleomycininduced mouse pulmonary fibrosis model. Richter et al.[18] performed parallel DNA encoded library screens against DDR1 and DDR2 and developed the potent DDR1 inhibitor **5**, which possessed excellent kinome selectivity (including 64-fold selectivity over DDR2 in a biochemical assay). Although these compounds had achieved good selectivity, some of them still had strong inhibition on tumor related targets, such as KDR, FGFR and PDGFR. These made them good antitumor inhibitors but not suitable for IPF treatment which requires better security. Giving the important role of DDR1/2 in pulmonary fibrosis, selective DDRs inhibitors activity would be more demanded to investigate the biological functions of DDRs as well as its therapeutic value.

In this work, along with our previous work, we discovered a series of quinazoline derivatives targeting DDR2 with elevated selectivity through structure–activity relationship study and computer-aided drug design. Through the selectivity assay against a kinase diversity panel, compound **47** could effectively inhibit the enzymatic activity of DDR1/2, with weak inhibitory activities against other 50-plus kinases. Besides, in cytotoxicity test and *in vivo* pharmacodynamic evaluation, the tolerated dose of compound **47** was significantly higher than that of nintedanib (trade name: Ofev), a multi-kinase inhibitor used in IPF treatment, indicating good safety and better efficacy. In this work, we preliminarily proved that DDR1/2 could be the IPF drug target as it plays an important role in the fibrotic processes.
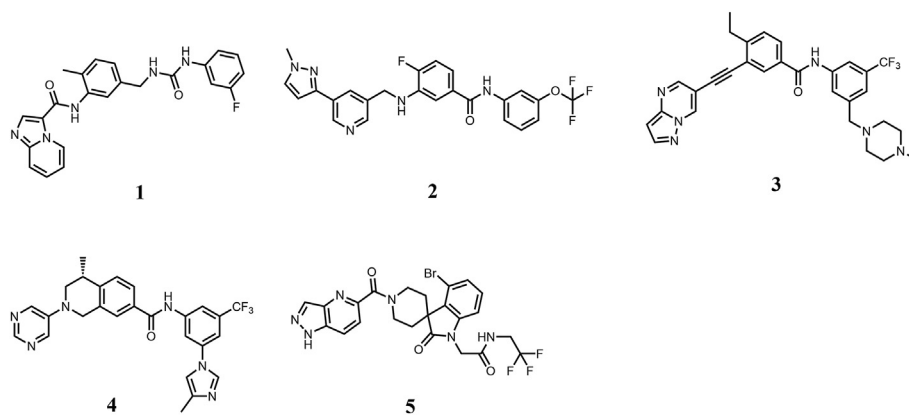
Figure 1 Chemical structures of reported DDR1/DDR2 inhibitors.

2. Results and discussion

2.1. Chemistry and structure analysis

Compounds were synthesized using the routes described in Schemes 1–4. A series of indazole derivatives as DDR2 inhibitors were discovered in our previous work for the treatment of lung squamous cell carcinoma[19]. Among them, compound **6** (Fig. 2A) was a potent, type-II kinase inhibitor that bound in the ATP pocket and extended into an allosteric region near the C-helix. This binding site is formed following a conformational change of the essential DFG loop (DFG-out). It was later confirmed to be a multi-kinase inhibitor targeting many tyrosine kinases. Although its multi-kinase targeting may have some advantages for anti-cancer drug development, it certainly is not appropriate for fibrosis-related diseases. Therefore, improving the selectivity of the compound **6** to reduce the off-targeting some kinases that were not reported to be involved in the process of pulmonary fibrosis would be of great importance of developing DDR inhibitors for IPF[20]. In addition, the indazole derivatives reported in the previous work demonstrated weak cellular activity, implying it might also suffer membrane permeability issue. Therefore, we launched chemical modifications with a bioisosterism strategy to overcome these undesirable properties.

2.2. Identification of quinazoline as the hinge binder with DDR2

Hinge-binding motif of kinase inhibitor is essential for the binding, as it can not only provide the anchor for the ligand located in the ATP binding site but also achieve some degree of selectivity for certain kinases. The bioisosteric replacement was first applied to the optimization of structure–activity relationship (SAR) of the hinge binding part. The docking study (Fig. 2A) showed the indazole motif in compound **6** could form two hydrogen bonds with Met657 and Glu655, thus we synthesized compounds **8–13** for study and also used compound **7** (reported in the previous work) as a reference compound (Table 1)[19]. Compound **8** was designed by using1,2-benzoxazole to replace the indazole, which converted the hydrogen bond donor NH to hydrogen bond acceptor O. Reduced activity of **8** indicated that NH of indazole indeed made additional contribution to the binding energy. Lactam scaffold of indolin-2-one **9** was thought to have the same binding mode as indazole motif with carbonyl much closer to Met657, which showed retained activity. Isochromane scaffold (**10**) adopted oxygen atom as hydrogen bond receptor interacting with the hinge. And decreased activity of it

implied the aromatic ring also played an important role in the activity. Isoquinoline fragment is a typical hinge binder, as it changed the ring electricity by introducing large heteroaromatic system with one nitrogen atom as hydrogen bond acceptor. Difference in activities on DDR2 inhibition were observed when isoquinoline rings were attached at different positions (**11** and **12**), which reinforced the hydrogen bonding acceptor of nitrogen atom played important role in the binding. Similarly, another common pharmacophore of ATP-competitive kinase inhibitors, the quinazoline scaffold, was adopted for the modification[21]. As expected, compound **13** showed potent inhibitory activity towards DDR2 kinase. Accordingly, compounds with an amino group attached to the C1 or C3 position of the quinazoline were synthesized to probe the possibilities of hydrogen bonding interaction between the amino group and the hinge (**14** and **15**). The assay showed that compound **15** had better activity than **14**. As the amino group of **15** was thought to stretch to the solvent-accessible region, it could be further modified to improve potency and drug-like properties. Then, more substitutions were introduced to the amine group of **15** to yield compounds **16–24**. Clearly, the optimization toward the solvent-accessible region was well tolerated. Compounds with different types of cyclic rings or varied length of the link moieties all showed potent activities with IC$_{50}$ value between 1 and 10 nmol/L except compound **19** which did not contain the hydrogen atom on the amino group and might sterically impede the interaction with the hinge part.

Although compound **11** showed best DDR2 activity in Table 1, the docking study suggested it might have a different binding mode with compound **6**. When the indazole scaffold of compound **6** was replaced by a quinazoline one, the activities of the compounds could also be well reserved. Compound **22** was subjected to docking study (Fig. 2B). We found the binding mode of this compound was similar to compound **6**, with the quinazoline ring interacted with hinge residue Met657 and the terminal amide group formed two hydrogen bonds with nearby residues Asp737 and Glu625. Compound **22** was then selected to test the kinase selectivity. Besides DDR2, compound **22** also strongly inhibited the enzymatic activities of KDR, VEGFR-1, PDGFR, EPH-A2, Ret, ABL, AXL, FGFR-1, ErbB4, and c-Src, with the inhibition ratio over 50% at 10 nmol/L, which was similar to compound **6**. However, the inhibition ratio on ALK of compound **22** decreased to 18.5% at 1 μmol/L while the inhibition of compound **6** was 93.5%, which indicated that the quinazoline scaffold might have some kinase selectivity. In the following work, efforts were made to improve the kinase selectivity towards the DDRs.
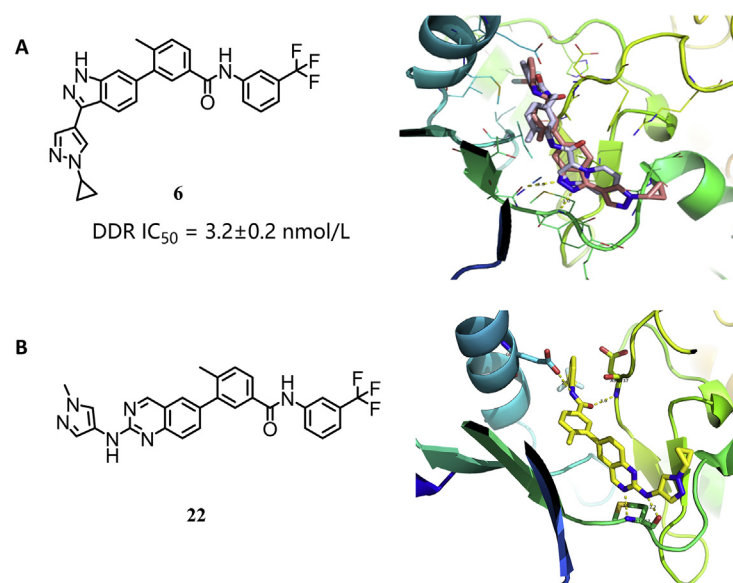
Figure 2 Docking study of compound **6** and **22** in the ATP binding site of DDR2, which is based on the protein model prepared from crystal structure 7AYM. (A) The chemical structure of **6** and the superimposition of the binding interaction of compounds **6** (colored in pink) and the original ligand (colored in grey). (B) Docking study of compound **22** (colored in yellow) in the ATP binding site of DDR2. The essential hydrogen bonding residues were shown in stick mode.
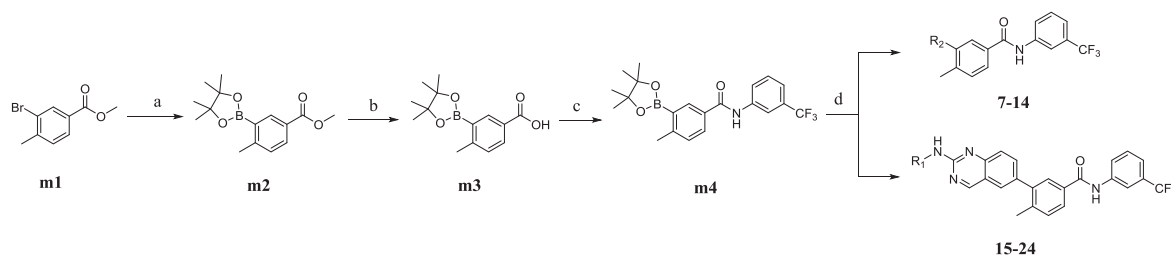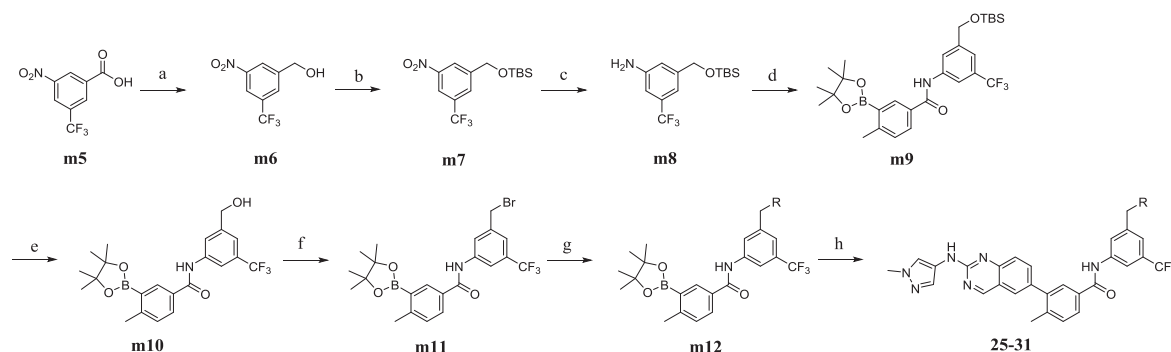

Scheme 1 Synthesis of compounds **7–24**. Reagents and conditions: (a) bis(pinacolato)diboron, Pd(dppf)$_2$Cl$_2$·CH$_2$Cl$_2$, AcOK, DMSO, 80 °C; (b) LiOH·H$_2$O, THF, H$_2$O, 25 °C; (c) 3-trifluoromethylaniline, HATU, DIEA, DMF, 25 °C; (d) corresponding halogenated aromatic hydrocarbon, Pd(dppf)$_2$Cl$_2$·CH$_2$Cl$_2$, K$_2$CO$_3$, 1,4-dioxane, H$_2$O, 80 °C.

2.3. Optimization of hydrophilic part

According to the docking result, the trifluoromethylphenyl part stretched to the allosteric region under DGF-out conformation of DDR2. Based on the previous SAR, this part could improve DDR2 inhibitory activity. Therefore, we introduced piperazinyl groups to the terminal phenyl group (**25–29**) to investigate their effects on DDR2 potency and selectivity (Table 2). Inhibition on

Scheme 2 Synthesis of compounds **25–31**. Reagents and conditions: (a) B$_2$H$_6$·THF, dried THF, 0–25 °C; (b) TBSCl, 1H-imidazole, dried dichloromethane, 25 °C; (c) Pd/C, ethanol, 25 °C; (d) **m3**, HATU, DIEA, N,N-dimethylformamide, 25 °C; (e) tetrabutylammonium fluoride, dried THF, 25 °C; (f) triphenylphosphine, carbon tetrabromide, dried dichloromethane, 25 °C; (g) corresponding nucleophile reagent, dried dichloromethane, triethylamine, 25 °C; (h) Pd(dppf)$_2$Cl$_2$·CH$_2$Cl$_2$, K$_2$CO$_3$, 1,4-dioxane, H$_2$O, 80 °C.
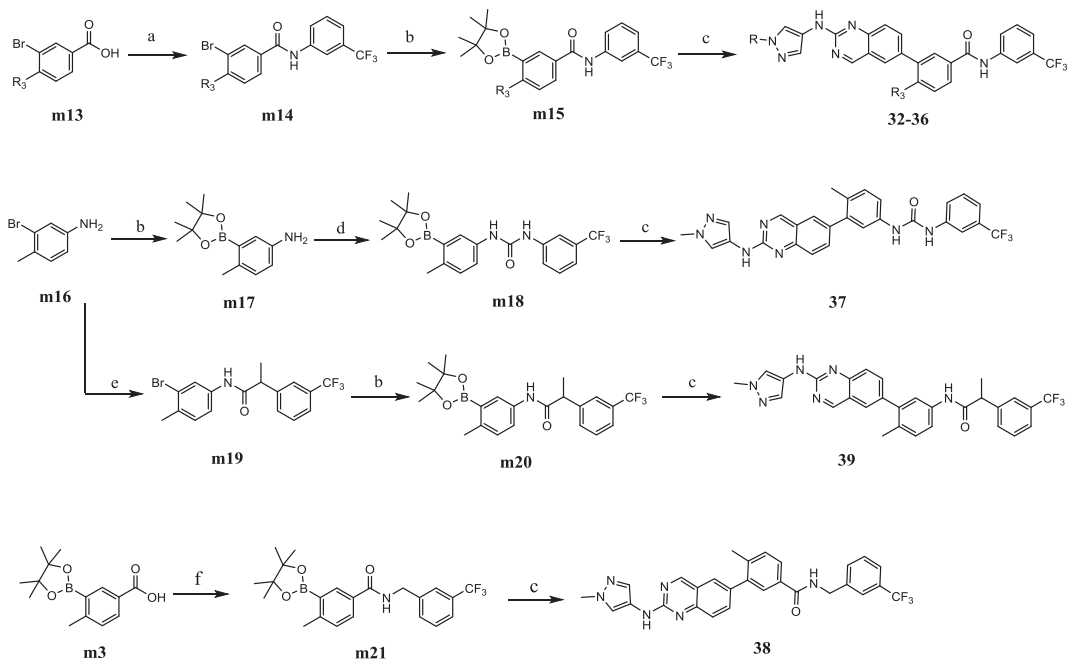
Scheme 3 Synthesis of compounds **32–39**. Reagents and conditions: (a) 3-trifluoromethylaniline, HATU, DIEA, DMF, 25 °C; (b) bis(pinacolato)diboron, Pd(dppf)$_2$Cl$_2$·CH$_2$Cl$_2$, AcOK, DMSO, 80 °C; (c) corresponding halogenated aromatic hydrocarbon, Pd(dppf)$_2$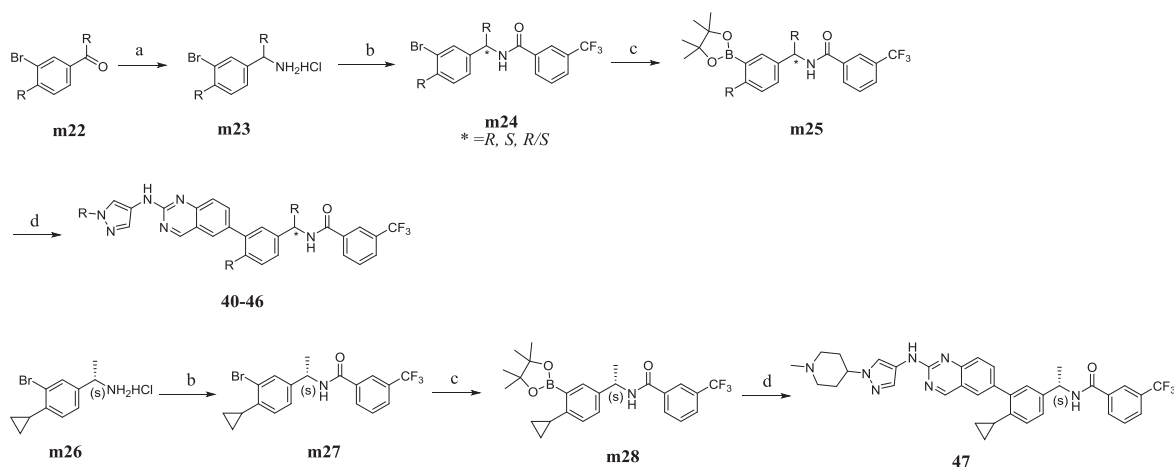Cl$_2$·CH$_2$Cl$_2$, K$_2$CO$_3$, 1,4-dioxane, H$_2$O, 80 °C; (d) 1-isocyanato-3-(trifluoromethyl) benzene, dried THF, 25 °C; (e) 2-(3-(trifluoromethyl)phenyl)propanoic acid, HATU, DIEA, DMF, 25 °C; (f) (3-(trifluoromethyl)phenyl)methanamine, HATU, DIEA, DMF, 25 °C.

RET and Flt3 was used to monitor the kinase selectivity. To investigate the cavity of this region, different size of substituents ranging from methyl to cyclopentyl were introduced to piperazinyl (**25–27**). IC$_{50}$ value of these compounds were within 1−5 nmol/L, which indicated the depth of the region was big enough. Hydrogen bond receptor such as acetyl group (**28**) was introduced to verify the additional hydrogen-bond interaction. Attachment of hydrophobic groups, such as methyl, to the piperazinyl (**29**) maintained strong inhibitory activity. Besides piperazinyl, other carbon heterocycles, such as diazepanyl (**30**) and bridged-ring (**31**), were also employed. They both showed potent inhibition with IC$_{50}$ value below 5 nmol/L, which

indicated the region had enough width to contain these structures. However these compounds all showed high inhibitions on RET and Flt-3. Therefore, further optimization would be focused on other parts of the scaffold.

2.4. Optimization of the "flag methyl"

In our previous work we found modification of "flag methyl" would influence activity and selectivity[19]. We chose different size of substituents to replace the methyl group, such as ethyl (**32**), methoxyl (**33**), isopropyl (**34**) and cyclopropyl (**35**). These compounds maintained good inhibitory activities toward DDR2

Scheme 4 Synthesis of compounds **12d–k**. Reagents and conditions: (a) CH$_3$COONH$_4$, NaBH$_3$CN, MeOH, 25 °C; (b) 3-(trifluoromethyl) benzoic acid, HATU, DIEA, DMF, 25 °C; (c) bis(pinacolato) diboron, Pd(dppf)$_2$Cl$_2$·CH$_2$Cl$_2$, AcOK, DMSO, 80 °C; (d) Pd(dppf)$_2$Cl$_2$·CH$_2$Cl$_2$, K$_2$CO$_3$, 1,4-dioxane, H$_2$O, 80 °C.

Table 1   SAR of initial optimization of the hinge binder (compounds **7–24**)[a].

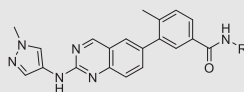| No.	Ar	DDR2 IC$_{50}$ (nmol/L)	No.	Ar	DDR2 IC$_{50}$ (nmol/L)
7		1.5 ± 0.1	16		9.9 ± 1.0
8		66.3 ± 9.3	17		10.5 ± 1.0
9		4.9 ± 1.1	18		3.4 ± 0.7
10		20.9 ± 5.2	19		42.4 ± 2.3
11		1.6 ± 0.1	20		5.7 ± 0.3
12		36.5 ± 1.0	21		6.3 ± 0.5
13		2.6 ± 0.1	22		2.2 ± 0.1
14		3.8 ± 0.2	23		6.5 ± 1.5
15		1.9 ± 0.4	24		2.8 ± 0.5

[a]Positive control: dasatinib DDR2, IC$_{50}$ = 1.0 ± 0.02 (reported 4.8 nmol/L).

comparing to **22**, while the activities of RET and Flt3 went down with the rise of substituents' size, among which **35** reduces the RET and Flt3 activities by nearly a half. These results indicated that the "flag methyl" part did affect activity and selectivity. According to compound **6**, the replacement of methyl group on pyrazole by a cyclopropyl one significantly improved the pharmacokinetic properties, thus we synthesized compound **36** and surprisingly found this optimization further reduced the activities against RET and Flt3 (Table 3).

2.5.   Optimization of the amide group

Compared to **22**, compound **36** had a significant improvement in kinase selectivity. Among the 33 tested kinases, only ABL and KDR were inhibited over 50% at 10 nmol/L, which gave us confidence for further optimization. We turned to the amide part and found it was tolerated when replaced by the structure of urea (**37**, Table 4). Since urea usually causes low solubility, we replaced one of the NH groups with a methylene (**38**) to keep the length of the structure. Considering that methylene may be a potential metabolic site, we introduced a methyl group to block the site. Together, by changing the chemical bond order, we synthesized compounds **39** and **40**. The results showed that the

selectivity of compounds **39** and **40** against KDR were both higher than that of compound **36**. Compound **40** displayed better selectivity, which indicated more investigation should be conducted on the basis of **40**. When methyl was replaced by ethyl at R$_2$ group, it could be found that although the inhibitory activity of compound **41** against KDR was significantly reduced, the inhibitory activity against DDR2 was also reduced. When the methyl group in X part was substituted with an ethyl group, compound **42** showed similar activity to **40** and a slight weak activity on KDR. According to the results in Table 3, when cyclopropyl groups were used in R$_1$ and/or R$_2$, it was helpful to improve activity and selectivity. Therefore, we designed and synthesized compounds **43** and **44**. The results showed that the activities against KDR of **43** and **44** were both greatly reduced, however, the DDR2 inhibitory activity of **44** was also decreased. The X-part of compound **44** contained a chiral carbon atom and could be separated into compounds **45** and **46**. From the results we found the *S* configuration (**46**) was about 10-fold more potent than the *R* (**45**). Although the cyclopropyl group improved the pharmacokinetic properties, the hydrophobicity of **46** might be the reason of decreased activity of DDR2, hence, we introduced methylpiperidinyl as a hydrophilic group to get compound **47**. The activity of **47** had an obvious increase compared to **46** while the selectivity of KDR remained.

Table 2 SAR of the optimization of hydrophilic part (compounds **25–31**).

No.	R	DDR2 IC$_{50}$ (nmol/L)	RET[a] inhibition @10 nmol/L[a]	Flt-3[a] inhibition @10 nmol/L[a]
25		1.7 ± 0.3	93.9%	93.5%
26		2.2 ± 0.3	92.7%	90.1%
27		3.1 ± 1.0	92.8%	94.4%
28		1.8 ± 0.1	91.8%	92.4%
29		2.7 ± 0.2	91.6%	93.8%
30		2.8 ± 0.2	93.2%	97%
31		2.9 ± 0.2	95%	96%

[a]The inhibition values are shown as the mean value from two separate experiments.

2.6. Assessment of fibroblast activation inhibition

We selected several compounds with potent DDR2 inhibition to investigate their inhibitory activities at cellular level. Their effects on the phosphorylation of DDR2 and cellular effects in MRC-5 cell lines were analyzed. After 24 h of TGF-β stimulation, the selected compounds were found to exhibit high inhibitory activity against DDR2 phosphorylation at 1 μmol/L, especially compounds **22**, **24**, **36** and **47**. In addition, the expression levels of α-SMA and fibronectin which are fibrosis markers were also examined. Results showed that compound **47** possessed a prominent ability to impede fibroblast activation and ECM deposition at the cellular level, which was better than **36** and **46**. These results showed that these series of compounds had anti-fibrosis activities and indicated that these compounds could restrain TGF-β induced myofibroblast differentiation as DDRs inhibitors.
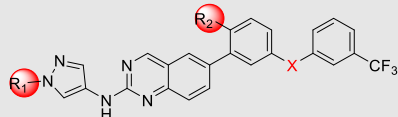
2.7. Kinase selectivity of compound 47
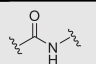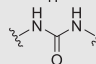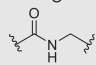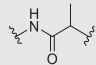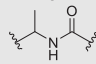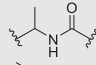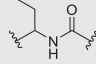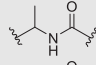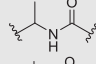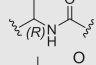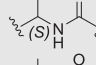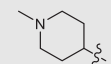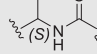
Nintedanib as a multikinase inhibitor affects three major signaling pathways involved in angiogenesis, which narrowed its safety window[22]. In previous tests compound **47** exhibited good activity and selectivity. Therefore, it was chosen for selectivity evaluation on a diversity kinase panel. Among the tested 60 kinases, only six

Table 3 SAR of the optimization of the flag methyl (compounds **22, 32–36**).
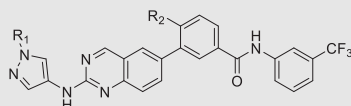
No	R$_1$	R$_2$	DDR2 IC$_{50}$ (nmol/L)	RET[a] inhibition @100 nmol/L[a]	Flt-3[a] inhibition @100 nmol/L[a]
22	Me	Me	2.2 ± 0.1	97.2%	80.3%
32	Me	Et	4.1 ± 0.7	77.1%	61.8%
33	Me	OMe	2.3 ± 0.5	41.3%	59.7%
34	Me	i-Pr	5.4 ± 0.4	54.5%	56.8%
35	Me	cPr	4.3 ± 0.7	50.7%	37.1%
36	cPr	cPr	6.1 ± 0.5	−18.6%	0%

[a]The inhibition values are shown as the mean value from two separate experiments.

Table 4   Lead optimization (compounds **36–47**).

No.	R_1	R_2	X	DDR2 IC_{50} (nmol/L)	KDR inhibition @100 nmol/L[a]
36	cPr	cPr	(structure)	6.1 ± 0.5	100%
37	CH_3	CH_3	(structure)	6.6 ± 0.4	89.3%
38	CH_3	CH_3	(structure)	1.3 ± 0.2	94%
39	CH_3	CH_3	(structure)	2.2 ± 0.2	70.2%
40	CH_3	CH_3	(structure)	4.1 ± 0.1	57.8%
41	CH_3	CH_2CH_3	(structure)	14.6 ± 3.3	31.0%
42	CH_3	CH_3	(structure)	5.0 ± 0.5	42.8%
43	cPr	CH_3	(structure)	4.3 ± 1.0	26.9%
44	cPr	cPr	(structure)	35.5 ± 3.9	28.8%
45	cPr	cPr	(R) (structure)	336.2 ± 108.3	49.1%
46	cPr	cPr	(S) (structure)	31.0 ± 5.8	24.2%
47	(piperidine structure)	cPr	(S) (structure)	8.2 ± 2.3	27.1%

[a]The inhibition values are shown as the mean value from two separate experiments.

kinases were inhibited over 50%@1 µmol/L by compound **47** (Fig. 4, Table 5). Compound **47** strongly inhibited ABL, EphA5 and EphB4 with over 90% inhibition at 1 µmol/L. Comparably, it had weak inhibition on PDGFR, FGFR and KDR, which might avoid toxicity issues associated with nintedanib. We also chose some compounds with high DDR2 activities to test their DDR1 inhibition. Compounds **6**, **7**, **22**, **24**, **36** and **47** showed strong inhibition on DDR1 with IC_{50} value of 14.11, 9.74, 8.13, 13.80, 16.04 and 2 nmol/L, respectively, which confirmed these compounds as DDRs inhibitors. When compared to the compounds in Fig. 1, **47** showed different kinase selective characteristics. Compounds **1** and **2** inhibited a number of other kinases besides DDR1/2, including KDR and PDGFR which might cause unwanted toxicity[14,15], while compound **47** had little inhibition activities on these kinases. Compounds **3–5** were actually DDR1 selective inhibitors[16–18]. Their selectivity of DDR1 over DDR2 were about 15−64 times while compound **47** was about 4 times. As stated before, DDR1 was a collagen activated receptor tyrosine kinase and might act as a mediator of the stromal−epithelial interaction, potentially controlling the activation state of the resident quiescent fibroblasts. Both DDR1 and DDR2 were thought to play pathogenic roles in organ fibrosis. And also there were reported study that collagen I could induce DDR1 expression

through DDR2 and a JAK2-ERK1/2-mediated mechanism in primary human lung fibroblasts[12], we suggested that increased portion of DDR2 activity might achieve better treatment effects. Thus we chose compound **47** for further study to evaluate the safety and anti-fibrosis effects *in vivo*.

2.8.   Pharmacokinetics assessment

Before *in vivo* pharmacological study, compound **47** was selected for pharmacokinetic assessment on mice (Table 6). Given *po* 10 and 100 mg/kg of **47**, the C_{max} were 217 ± 34 and 986 ± 195 ng/mL, respectively, which showed dose-dependent PK properties. Although the value of C_{max} was not high, the clearance rate of **47** in mice was low, which resulted in long $t_{1/2}$ and high AUC. Given iv 3 mg/kg of **47** the oral bioavailability was calculated as 16.9%. Obviously **47** was oral-available, however, there was a mismatch between the dose and the C_{max} value. To explain this phenomenon, **47** was subjected to tissue distribution investigation (Table 7). Compared to low plasma concentration, **47** showed favorable tissue distribution especially in lung, kidney and liver as these were also main target tissues for fibrosis treatment (Table 7). Since **47** accumulates in the lungs and kidneys, in order to rule out its damage to these two organs, we
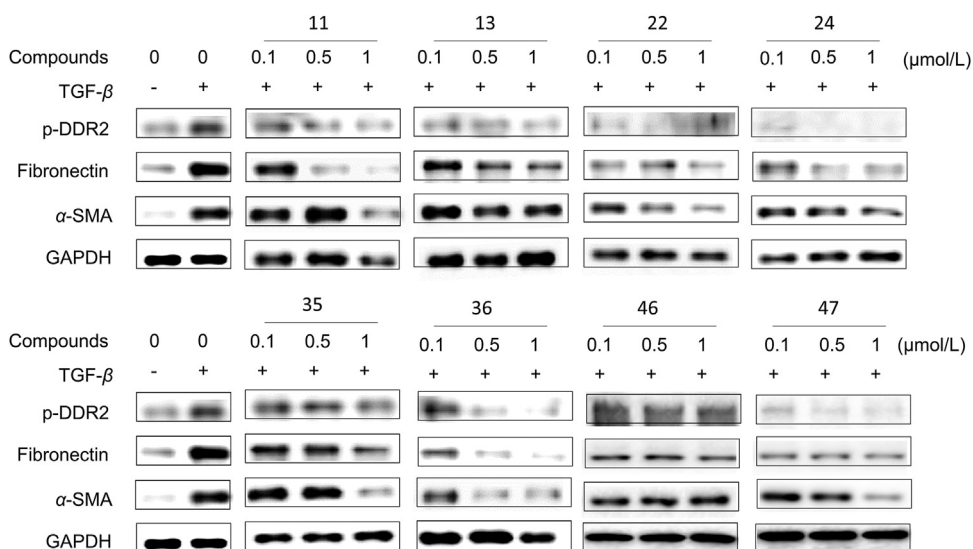
Figure 3 Assessment of fibroblast activation inhibition of MRC-5 for select compounds. Confluent MRC-5 were stimulated with TGF-β (5 ng/mL) and treated with different concentrations of indicated compounds for 24 h. Representative Western blots of P-DDR2 Fibronectin, α-SMA and GAPDH were shown.

conducted a 14-day subacute toxicity test, The results from the organ coefficient and HE slice show that **47** has no obvious toxicity to the lung and kidney at the two doses of 100 and 300 mg/kg (Supporting Information Fig. S1). At 0.25 h, the concentration in lung was about 10 times to heart plasma while at 8 h it increased to over 20 times, indicating a good exposure and long duration in lung. Therefore, it may provide high potential for the treatment on lung fibrosis.

2.9. Compound **47** inhibits TGF-β1 induced lung fibroblasts activation

From the previous data in Fig. 3, it could be seen that **47** dose-dependently inhibited the activation of lung fibroblast MRC-5 cells. Besides the effect at protein level in Fig. 3, q-PCR was used to detect the expression of genes associated with fibrosis such as fibronectin, α-SMA, TGF-β, TIMP-1 and MMP2 (Fig. 5A–E), which were inhibited by co-treatment with **47**. In order to truly reflect the effect of **47** on fibroblasts activation, we separated primary lung fibroblasts. As it shows in Fig. 5F, compound **47** could also inhibit primary lung fibroblasts activation in a dose-
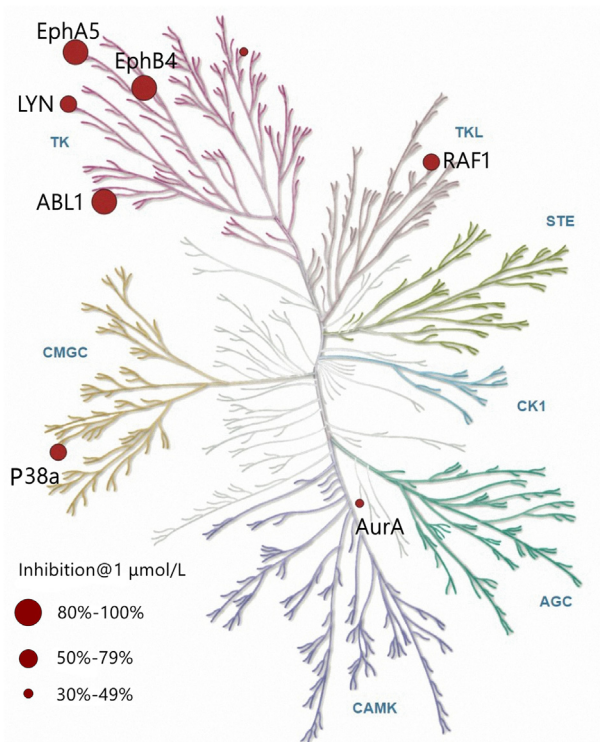
Figure 4 Selectivity assessment of compound **47** against 60 kinases.

Table 5 Kinases inhibition of compound **47** at 1 μmol/L.

Kinase	Inhibition @ 1 μmol/L (%)
ABL	94
EphB4	94
EphA5	90
P38a/SAPK2a	67
Lyn	66
c-RAF	59
AMPKα1, ASK1, aurora-A, CaMKI, CDK 1/cyclinB, CDK2/cyclinA, CDK6/ cyclinD3, CDK7/cyclinH/MAT1, CDK 9/cyclinT1, CHK1, CK1γ1, CK2α2, DRAK1, eEF-2K, EGFR, FGFR1, FGFR2, Fyn, GSK3β, IGF-1R, IKKα, IRAK4, JAK2, KDR, LOK, MAPKAP-K2, MEK1, MLK1, Mnk2, MSK2, MST1, mTOR, NEK2, p70S6K, PAK2, PDGFRα, PDGFRβ, PI3 kinase (p110a/ p85a), PI3 kinase (p110b/p85a), PI3 kinase (p110d/p85a), PI3 kinase (p120g), Pim-1, PKA, PKBα, PKCα, PKCθ, PKG1α, Plk3, PRAK, ROCK-I, Rse, Rsk1, SRPK1, TAK	<50

Table 6   Plasma-derived PK parameters of **47** in mice with multiple doses[a].

Property	**47** (*po*)		**47** (*iv*)
	10 mg/kg	100 mg/kg	3 mg/kg
$t_{1/2}$ (h)	4.05	18.3 ± 5.59	4.99 ± 1.47
T_{max} (h)	4	5.33 ± 2.31	–
C_{max} (ng/mL)	217 ± 34	986 ± 195	–
AUC_{last} (h·ng/mL)	2045 ± 260	$15,570 \pm 3480$	3117 ± 762
AUC_{INF_obs} (h·ng/mL)	2093 ± 271	$29,091 \pm 10,774$	3708 ± 425
MRT_{INF_obs} (h)	8.68 ± 0.15	29.3 ± 7.40	5.84 ± 0.73
$CL_{\_obs}$ (mL/min/kg)	–	–	13.6 ± 1.56
$F\%$	16.9		

[a]Formulation: DMAC/0.5% methylcellulose (5:95, *v/v*); AUC = area under the curve; C_{max} = maximal concentration; MRT = mean residence time; $t_{1/2}$ = half-life. Only representative PK data are listed here. Linear dose dependency and no sex effect was observed.

Table 7   Tissue distribution of **47** in mice (10 mg/kg, *po*).

Time (h)	Heart plasma Conc. (ng/mL)	Portal vein plasma Conc. (ng/mL)	Brain Conc. (ng/g)	Lung Conc. (ng/g)	Liver Conc. (ng/g)	Kidney Conc. (ng/g)	Thymus Conc. (ng/g)
0.25	39.07 ± 21.40	82.60 ± 34.69	BLQ[a]	476.67 ± 161.68	1519.33 ± 502.30	397.67 ± 170.52	42.53 ± 14.94
8	177.33 ± 42.28	159.33 ± 26.13	25.83 ± 4.02	4366 ± 894	3132.67 ± 639.75	3218.67 ± 752.56	887.67 ± 213.11

[a]BLQ: beneath limit of quantification.
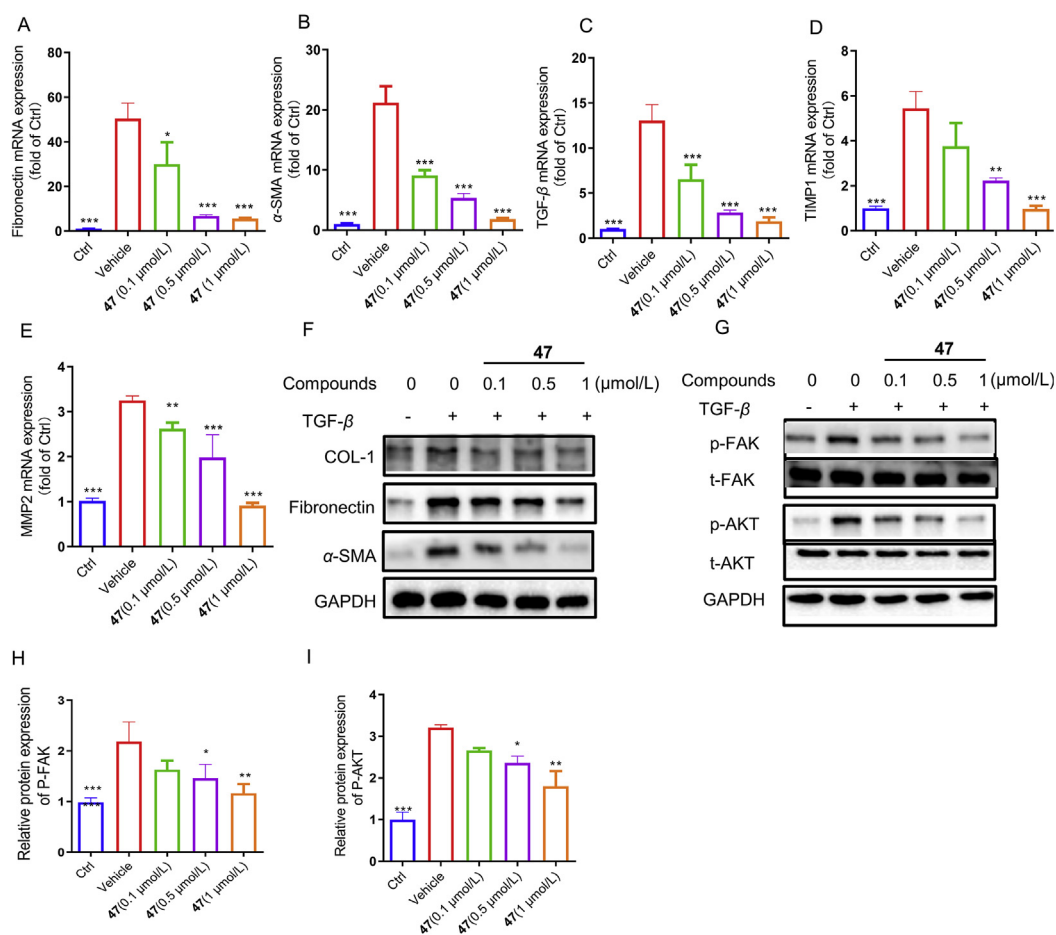
Figure 5   Compound **47** limits TGF-β induced lung fibroblast to myofibroblast transition. (A)–(E) Confluent MRC-5 were stimulated with TGF-β (5 ng/mL) and treated with different concentrations of **47** for 24 h. Fibronectin, α-SMA, TGF-β, TIMP1, MMP2 expression were analyzed by qPCR. (F) Mouse primary fibroblasts were incubated with TGF-β (5 ng/mL) and treated with different concentrations of **47** for 24 h. Fibronectin, COL1 and α-SMA expression were analyzed by Western blotting. (G) p-FAK, t-FAK, p-AKT, t-AKT expression were analyzed by Western blotting. (H) and (I) Quantitative analysis showed the fold change of these phosphorylation levels in panel G. Bar groups represent the mean $\pm$ SEM; The statistical significance was compared with the vehicle group with one-way ANOVA followed by fisher's LSD tests. *$P < 0.05$, **$P < 0.01$, ***$P < 0.001$.
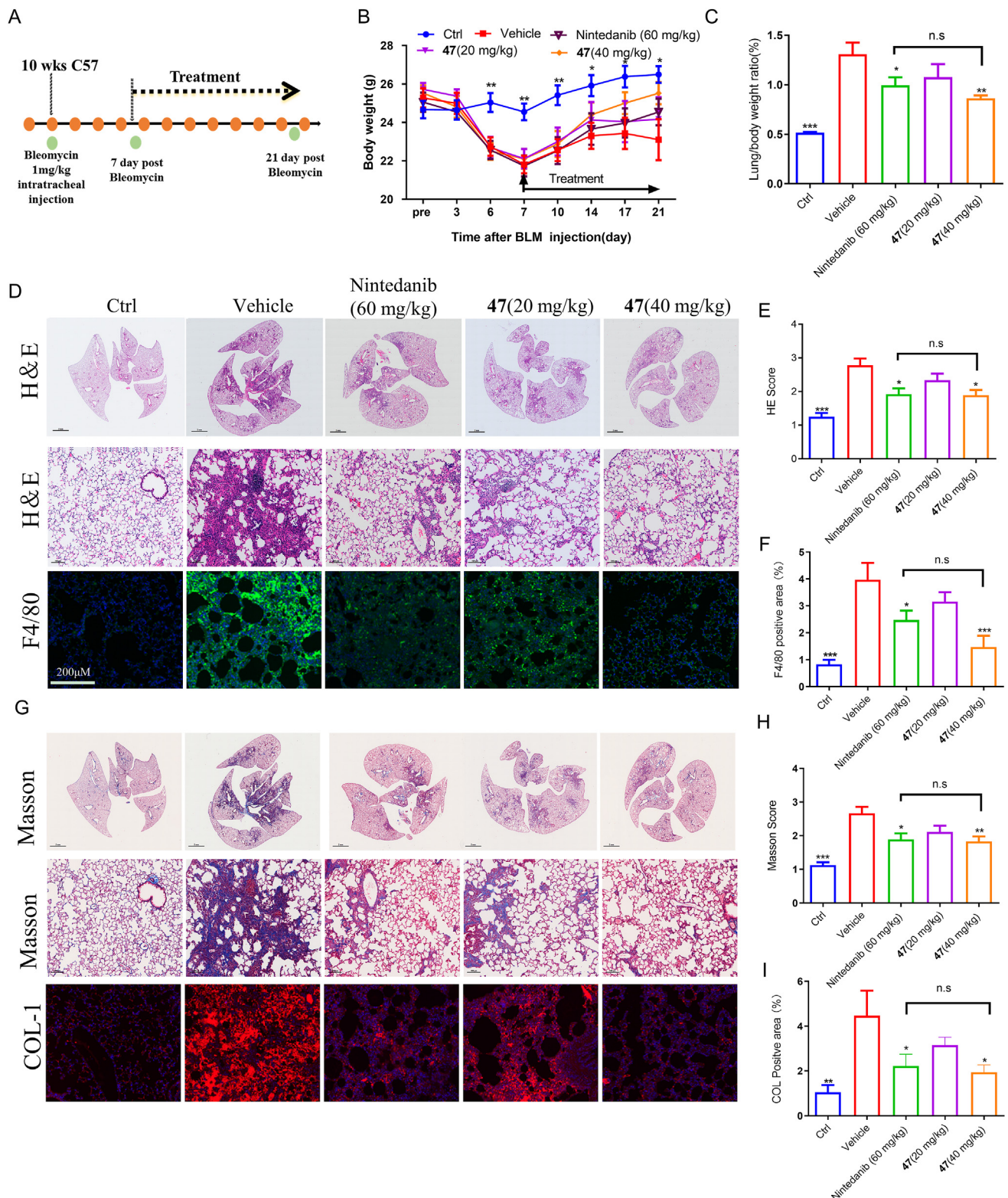
Figure 6 Effect of **47** on BLM induced mouse lung fibrosis. Mice were intratracheal instilled with BLM (1.7 U/kg) or with saline only for 7 days. Then the indicated dose (mg/kg) of **47** and nintedanib were given once daily for 21 days ($n = 6{-}9$ per group). (A) Schematic diagram of animal experiments. (B) Body weight change chart of different groups in 21 days of experimental period. (C) The lung/body weight ratio. (D) Section of lung tissue was prepared on Day 21 after BLM treatment and subjected to H&E and F4/80 staining. (E) The score of HE staining. (F) Fluorescence quantification of F4/80 staining. (G) Masson and COL-1 (collagen-a1) staining. (H) The score of MASSON staining. (I) Fluorescence quantification of COL-1 staining Data were analyzed with one-way ANOVA, followed by fisher's LSD tests with two tailed distribution. Bar groups represent the mean $\pm$ SEM; $*P < 0.05$, $**P < 0.01$, $***P < 0.001$.

dependent manner from 0.1 to 1 μmol/L. Next, we tried to explore the molecular pathway underlying compound **47** regulation of lung myofibroblast biology. The phosphorylation levels of major downstream mediators of TGF-β were analyzed. Compared with control MRC-5, TGF-β treatment resulted in the increase of the phosphorylation levels of AKT and FAK, while compound **47** could significantly reduce p-AKT, p-FAK to 53 ± 7.4%, 51 ± 7.5% respectively (Fig. 5H and I). These results revealed that **47** might inhibit the activation of myofibroblasts during lung fibrosis through inhibiting the TGF-β induced activation of AKT and FAK.

2.10. Notable therapeutic effects of compound 47 against lung fibrosis in preclinical animal model

Due to the excellent cell activity and *in vivo* pharmacokinetic properties of **47**, we next evaluated the *in vivo* anti-fibrosis potential of **47** in the bleomycin-induced pulmonary fibrosis models of mice and rat. The study design on mice was shown in Fig. 6A. In the therapeutic regimen experiment, the body weight of mice in each group decreased in the first six days and began to recover on the seventh day (Fig. 6B). The weight of mice at

the end of the treatment were 26.5 ± 1.07, 23.1 ± 3.2, 24.54 ± 2.09, 24.17 ± 3.43 and 25.52 ± 1.73 g in the control, vehicle, 60 mg/kg nintedanib, and **47** (20, 40 mg/kg) groups, respectively. The weight recovery ratio of mice in **47** (40 mg/kg) treatment group (15.48%) was better than 60 mg/kg nintedanib group (12.93%). Similar results were observed on the lung/body weights ratios of mice (Fig. 6C). H&E staining of whole lung tissues were performed to evaluate pulmonary injury and inflammation. HE scores was greatly reduced from 2.778 ± 0.202 to 1.889 ± 0.156 by **47** (40 mg/kg). The degree of reduction is similar to that of 60 mg/kg nintedanib. Immunofluorescence staining for the cell surface maker of F4/80 was used to indicate the infiltrating macrophages. As shown in Fig. 6D, treatment of **47** reduced the accumulation of infiltrating macrophages in the lung tissues, which suggested anti-inflammatory effects of **47** in the bleomycin-induced lung injury. The Masson scores, indicating as fibrosis degree, in the **47** (40 mg/kg) and nintedanib (60 mg/kg) treatment groups were significantly decreased from 2.67 ± 0.57 (vehicle) to 1.83 ± 0.43 and 1.89 ± 0.55, respectively. Immunofluorescence of COL-1 also confirmed that the extracellular matrix was greatly improved by **47**. The rat model of unilateral pulmonary
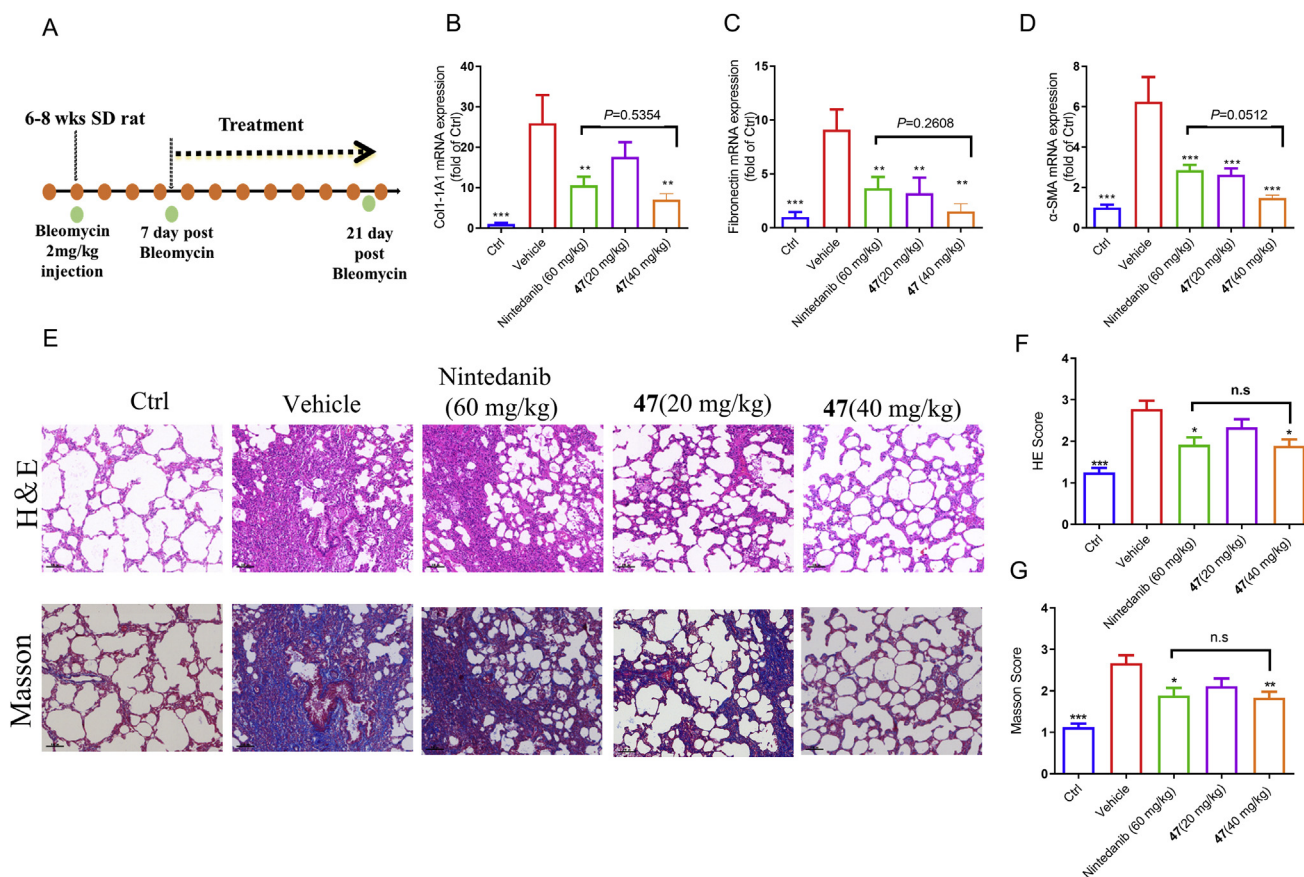
Figure 7 Effect of 47 on BLM induced rat lung fibrosis. Rats were unilateral intratracheal instilled with BLM (3.4 U/kg) or with saline only for 7 days, Then the indicated dose (mg/kg) of **47** and nintedanib were given once daily for 14 days (*n* = 6−7 per group). (A) Schematic diagram of animal experiments. (B−D) mRNA levels of various fibrosis associated markers, including COL-1, fibronectin, and α-SMA, were determined as described in the methods. (E) Section of left lung tissue was prepared on day 21 after BLM treatment and subjected to H&E and MASSON staining. (F) The score of H&E staining. (G) The score of MASSON staining. Bar groups represent the mean ± SEM; The statistical significance was compared with the vehicle group with one-way ANOVA followed by fisher's LSD tests. *$P < 0.05$, **$P < 0.01$, ***$P < 0.001$.

fibrosis has gradually become a principal animal model before the clinical application of new drugs for pulmonary fibrosis due to its appealing stability and low mortality (Fig. 7A). The results showed that **47** (20 and 40 mg/kg) could concentration-dependently reduce the mRNA levels of COL-1, Fibronectin and α-SMA which serve as ECM deposition and fibroblast activation marker (Fig. 7B−D). Especially under the concentration of 40 mg/kg, the anti-fibrosis effect of **47** had better inhibitory effect on fibrosis markers mentioned above than that of nintedanib at 60 mg/kg. H&E and MASSON staining also collaboratively demonstrated that **47** had better anti-fibrosis and anti-lung injury efficacy than nintedanib (Fig. 7E−G). Therefore, administration of **47** reduced BLM induced pulmonary fibrosis which even showed better efficacy than nintedanib.

3. Conclusions

The U.S. Food and Drug Administration (FDA) had approved two drugs for the treatment of IPF: pirfenidone and nintedanib. Both drugs reduced the progression of IPF and offered survival benefit. However, no treatment is strongly recommended for patients with IPF. Problems in accurate diagnosis along with poor prognosis limit the clinical therapy, and high mortality rate clearly demonstrate the need to develop efficient therapeutic strategies for IPF. Discoidin domain receptors were reported as potentially effective targets for treatment of pulmonary fibrosis including IPF. Their unique ligands (collagens) and prolonged active mechanism implied a different strategy for the treatment of IPF. In this work, through extensive optimization of our previous multi-kinase inhibitors, we discovered a series of more selective DDRs inhibitors. Among them, compound **47** showed potent activity against DDR1/2 and reduced activities of PDGFR, FGFR and KDR, which made it less toxic than nintedanib. *In vivo* assessment showed that compound **47** attenuated BLM-induced lung injury, inflammation and pulmonary fibrosis, which exhibited similar effects to nintedanib and even better on some indicators. Besides, **47** could also curb the activation of myofibroblasts during lung fibrosis through inhibiting the TGF-β induced activation of AKT and FAK. Therefore, compound **47** was a promising DDRs inhibitor that advanced into further drug development.

4. Experimental

4.1. General information

^{1}H NMR (400 MHz) spectra were recorded with a Varian Mercury-400 High Performance Digital FT-NMR spectrometer with tetramethylsilane (TMS) as an internal standard. ^{13}C NMR (100 or 125 MHz) spectra were recorded by using a Varian Mercury-400 High Performance Digital FT-NMR spectrometer or Varian Mercury-500 High Performance Digital FT-NMR spectrometer. Abbreviations for peak patterns in NMR spectra: br = broad, s = singlet, d = doublet, and m = multiplet. Low-resolution mass spectra were obtained with a Finnigan LCQ Deca XP mass spectrometer using a CAPCELL PAK C18 (50 mm × 2.0 mm, 5 μm) or an Agilent ZORBAX Eclipse XDB C18 (50 mm × 2.1 mm, 5 μm) in positive or negative electrospray mode. Low-resolution mass spectra and high-resolution mass spectra were recorded at an ionizing voltage of 70 eV on a Finnigan/MAT95 spectrometer. High-resolution mass spectra were recorded by using a Finnigan MAT-95 mass spectrometer or an Agilent technologies 6224 TOF mass spectrometer. Purity of all compounds was determined by analytical Gilson high-performance liquid chromatography (HPLC) using an YMC ODS3 column (50 mm × 4.6 mm, 5 μm). Conditions were as follows: CH$_3$CN/H$_2$O eluent at 2.5 mL/min flow [containing 0.1% trifluoroacetic acid (TFA)] at 35 °C, 8min, gradient 5% CH$_3$CN to 95% CH$_3$CN, monitored by UV absorption at 214 and 254 nm. TLC analysis was carried out with glass precoated silica gel GF254 plates. TLC spots were visualized under UV light. Flash column chromatography was performed with a Teledyne ISCO CombiFlash Rf system. All solvents and reagents were used directly as obtained commercially unless otherwise noted. Anhydrous dimethylformamide was purchased from Acros and was used without further drying. All air and moisture sensitive reactions were carried out under an atmosphere of dry Argon with heat-dried glassware and standard syringe techniques.

4.2. Synthesis

4.2.1. General procedure A for the preparation of compounds 7–15
To a resealable vial was added K$_2$CO$_3$ (2 eq.), 4-methyl-3-(4,4,5,5-tetramethyl-1,3,2-dioxaborolan-2-yl)-*N*-(3-(trifluoromethyl) phenyl) benzamide (**m4**, 1 eq.), and corresponding halogenated heterocycles (1 eq.). The vial was evacuated and purged with Ar before addition of PdCl$_2$(dppf)-CH$_2$Cl$_2$ adduct (5%, *mol/mol*) and degassed 1,4-dioxane/water (4:1, *v/v*). The vial was sealed and heated to 80 °C overnight. The reaction was cooled to room temperature, which was then brought to saturated salt solution and extracted with ethyl acetate. The organic layer was collected and distilled under reduced pressure. The crude residue was purified *via* by silica gel column chromatography to afford the products.

4.2.2. 3-(1H-Indazol-6-yl)-4-methyl-N-(3-(trifluoromethyl) phenyl)benzamide (7)
White solid; yield: 82%. ^{1}H NMR (400 MHz, methanol-d_4) δ 8.19 (s, 1H), 8.13 (s, 1H), 7.95 (d, *J* = 8.2 Hz, 1H), 7.92 (m, 2H), 7.88 (d, *J* = 8.3 Hz, 1H), 7.57 (d, *J* = 7.9 Hz, 1H), 7.54 (s, 1H), 7.50 (d, *J* = 8.5 Hz, 1H), 7.44 (d, *J* = 8.7 Hz, 1H), 7.20 (d, *J* = 9.0 Hz, 1H), 2.38 (s, 3H). ^{13}C NMR (151 MHz, methanol-d_4) δ 168.73, 143.78, 141.51, 141.20, 140.93, 134.92, 133.35, 132.09 (d, *J* = 32.0 Hz), 131.77, 130.65, 130.19, 127.77, 125.58 (d, *J* = 271.5 Hz), 125.20, 123.83, 123.48, 121.66, 118.47 (d, *J* = 4.1 Hz), 111.35, 20.80. HRMS *m/z* (ESI) found 396.1313 [M+H]$^+$, C$_{22}$H$_{17}$F$_3$N$_3$O$^+$ Calcd. for 396.1318; HPLC 100% pure.

4.2.3. 3-(Benzo[d]isoxazol-6-yl)-4-methyl-N-(3-(trifluoromethyl)phenyl)benzamide (8)
Light green solid; yield: 76%. ^{1}H NMR (400 MHz, DMSO-d_6) δ 11.31 (s, 1H), 10.52 (s, 1H), 8.24 (s, 1H), 8.08 (d, *J* = 7.7 Hz, 1H), 7.96 (d, *J* = 7.6 Hz, 1H), 7.88 (s, 1H), 7.73 (d, *J* = 8.3 Hz, 1H), 7.61 (t, *J* = 7.9 Hz, 1H), 7.52 (d, *J* = 8.0 Hz, 1H), 7.46 (d, *J* = 7.6 Hz, 1H), 7.01 (s, 2H), 2.31 (s, 3H). ^{13}C NMR (126 MHz, DMSO-d_6) δ 165.62, 160.50, 147.29, 140.37, 139.52, 133.67, 132.46, 131.29, 130.32, 129.80 (d, *J* = 31.5 Hz), 128.60, 127.99, 124.62 (d, *J* = 272.4 Hz), 124.26, 121.07, 120.42, 120.39, 117.36, 117.09, 116.90, 116.87, 20.52. HRMS *m/z* (ESI) found 395.1007 [M−H]$^-$, C$_{22}$H$_{14}$F$_3$N$_2$O$_2^-$ Calcd. for 395.1013, HPLC >98% pure.

4.2.4. 4-Methyl-3-(2-oxoindolin-6-yl)-N-(3-(trifluoromethyl) phenyl)benzamide (9)

White solid; yield: 72%. ^{1}H NMR (400 MHz, DMSO-d_6) δ 10.51 (s, 1H), 10.50 (s, 1H), 8.25 (s, 1H), 8.08 (d, J = 8.6 Hz, 1H), 7.92 (d, J = 8.0 Hz, 1H), 7.87 (s, 1H), 7.60 (t, J = 7.9 Hz, 1H), 7.49 (d, J = 8.0 Hz, 1H), 7.46 (d, J = 7.6 Hz, 1H), 7.32 (d, J = 7.6 Hz, 1H), 6.97 (d, J = 7.5 Hz, 1H), 6.81 (s, 1H), 3.56 (s, 2H), 2.32 (s, 3H). ^{13}C NMR (126 MHz, DMSO-d_6) δ 176.95, 165.87, 144.35, 141.90, 140.45, 140.32, 139.69, 132.30, 131.04, 130.29, 129.03, 127.21, 125.41, 124.71, 124.63 (d, J = 272.2 Hz), 124.26, 122.49, 120.33, 116.90, 116.86, 110.15, 36.08, 20.70. HRMS m/z (ESI) found 409.1159 [M–H]$^-$, C$_{23}$H$_{16}$F$_3$N$_2$O$_2^-$ Calcd. for 409.1169, HPLC >98% pure.

4.2.5. 3-(Isochroman-7-yl)-4-methyl-N-(3-(trifluoromethyl) phenyl)benzamide (10)

White solid; yield: 75%. ^{1}H NMR (400 MHz, DMSO-d_6) δ 10.50 (s, 1H), 8.25 (s, 1H), 8.09 (d, J = 8.2 Hz, 1H), 7.90 (d, J = 8.0 Hz, 1H), 7.87 (s, 1H), 7.60 (t, J = 7.9 Hz, 1H), 7.46 (t, J = 8.4 Hz, 2H), 7.30−7.19 (m, 2H), 7.10 (s, 1H), 4.76 (s, 2H), 3.93 (t, J = 5.5 Hz, 2H), 2.85 (t, J = 5.4 Hz, 2H), 2.32 (s, 3H). ^{13}C NMR (126 MHz, DMSO-d_6) δ 165.91, 141.63, 140.47, 139.72, 138.53, 135.54, 132.70, 132.34, 131.00, 130.26, 129.79 (d, J = 31.5 Hz), 129.15, 127.48, 127.12, 125.49, 124.63 (d, J = 272.2 Hz), 124.23, 120.31, 116.87, 116.84, 67.59, 65.08, 27.98, 20.72. HRMS m/z (ESI) found 410.1369 [M–H]$^-$, C$_{24}$H$_{19}$F$_3$NO$_2^-$ Calcd. for 410.137, HPLC >98% pure.

4.2.6. 3-(Isoquinolin-7-yl)-4-methyl-N-(3-(trifluoromethyl) phenyl)benzamide (11)

White solid; yield: 75%. ^{1}H NMR (400 MHz, DMSO-d_6) δ 10.55 (s, 1H), 9.41 (s, 1H), 8.57 (d, J = 5.6 Hz, 1H), 8.25 (s, 1H), 8.21 (s, 1H), 8.10 (t, J = 8.1 Hz, 2H), 8.03 (s, 1H), 7.99 (d, J = 8.2 Hz, 1H), 7.94−7.89 (m, 2H), 7.61 (t, J = 8.2 Hz, 1H), 7.57 (d, J = 7.9 Hz, 1H), 7.46 (d, J = 8.3 Hz, 1H), 2.38 (s, 3H). ^{13}C NMR (126 MHz, DMSO-d_6) δ 165.82, 153.00, 143.56, 140.96, 140.42, 134.70, 132.56, 132.44, 131.26, 130.32, 129.80 (d, J = 31.5 Hz), 129.45, 128.65, 127.98, 127.73, 126.97, 124.63 (d, J = 272.3 Hz), 124.28, 120.66, 120.39, 120.37, 116.91, 116.87, 20.73 HRMS m/z (ESI) found 407.1371 [M+H]$^+$, C$_{24}$H$_{18}$F$_3$N$_2$O$^+$ Calcd. for 407.1366, HPLC >98% pure.

4.2.7. 3-(Isoquinolin-6-yl)-4-methyl-N-(3-(trifluoromethyl) phenyl)benzamide (12)

White solid; yield: 72%. ^{1}H NMR (400 MHz, DMSO-d_6) δ 10.55 (s, 1H), 9.41 (s, 1H), 8.57 (d, J = 5.7 Hz, 1H), 8.28−8.22 (m, 2H), 8.09 (d, J = 8.3 Hz, 1H), 8.05 (s, 1H), 8.02 (s, 1H), 8.00 (d, J = 9.4 Hz, 1H), 7.91 (d, J = 5.7 Hz, 1H), 7.79 (d, J = 8.5 Hz, 1H), 7.60 (t, J = 8.1 Hz, 1H), 7.56 (d, J = 8.1 Hz, 1H), 7.46 (d, J = 7.6 Hz, 1H), 2.37 (s, 3H). ^{13}C NMR (126 MHz, DMSO-d_6) δ 165.76, 152.66, 143.82, 143.07, 141.01, 140.41, 139.92, 135.66, 132.52, 131.26, 130.30, 129.80 (d, J = 31.6 Hz), 129.42, 129.33, 128.06, 127.87, 127.65, 126.85, 124.62 (d, J = 272.3 Hz), 124.27, 120.93, 120.37 (d, J = 3.6 Hz), 116.89 (d, J = 3.6 Hz), 20.69. HRMS m/z (ESI) found 407.1375 [M+H]$^+$, C$_{24}$H$_{18}$F$_3$N$_2$O$^+$ Calcd. for 407.1366, HPLC >99% pure.

4.2.8. 4-Methyl-3-(quinazolin-6-yl)-N-(3-(trifluoromethyl) phenyl)benzamide (13)

White solid; yield: 69%. ^{1}H NMR (400 MHz, DMSO-d_6) δ 10.56 (s, 1H), 9.69 (s, 1H), 9.37 (s, 1H), 8.26 (s, 1H), 8.25 (s, 1H), 8.15 (s, 2H), 8.09 (d, J = 8.1 Hz, 1H), 8.04 (s, 1H), 8.01 (d, J = 8.0 Hz, 1H), 7.60 (q, J = 8.0 Hz, 2H), 7.46 (d, J = 7.7 Hz, 1H), 2.39 (s, 3H). ^{13}C NMR (126 MHz, DMSO-d_6) δ 165.74, 161.31, 155.76, 148.91, 140.55, 140.39, 140.30, 140.00, 136.42, 132.64, 131.33, 130.31, 129.81 (d, J = 31.6 Hz), 129.47, 128.13, 127.95, 125.07, 124.62 (d, J = 272.3 Hz), 124.27, 120.39 (d, J = 3.6 Hz), 116.89 (d, J = 4.0 Hz), 20.69. HRMS m/z (ESI) found 408.1323 [M+H]$^+$, C$_{23}$H$_{17}$F$_3$N$_3$O$^+$ Calcd. for 408.1318, HPLC >99% pure.

4.2.9. 3-(4-Aminoquinazolin-6-yl)-4-methyl-N-(3-(trifluoromethyl)phenyl)benzamide (14)

White solid; yield: 69%. ^{1}H NMR (400 MHz, DMSO-d_6) δ 10.55 (s, 1H), 8.44 (s, 1H), 8.31 (s, 1H), 8.25 (s, 1H), 8.09 (d, J = 8.4 Hz, 1H), 8.00 (s, 1H), 7.97 (d, J = 9.4 Hz, 1H), 7.87 (d, J = 8.5 Hz, 2H), 7.77 (d, J = 8.5 Hz, 1H), 7.61 (t, J = 8.0 Hz, 1H), 7.55 (d, J = 8.0 Hz, 1H), 7.46 (d, J = 7.9 Hz, 1H), 2.39 (s, 3H). ^{13}C NMR (126 MHz, DMSO-d_6) δ 165.85, 162.30, 156.09, 149.18, 141.04, 140.43, 140.03, 138.04, 134.36, 132.49, 131.17, 130.33, 129.81 (d, J = 31.5 Hz), 129.53, 127.68, 127.56, 124.63 (d, J = 272.3 Hz), 124.28, 124.26, 120.38 (d, J = 3.9 Hz), 116.86 (d, J = 3.9 Hz), 114.64, 20.77. HRMS m/z (ESI) found 423.1427 [M+H]$^+$, C$_{23}$H$_{18}$F$_3$N$_4$O$^+$ Calcd. for 423.1427, HPLC >99% pure.

4.2.10. 3-(2-Aminoquinazolin-6-yl)-4-methyl-N-(3-(trifluoromethyl)phenyl)benzamide (15)

White solid; yield: 78%. ^{1}H NMR (400 MHz, DMSO-d_6) δ 10.53 (s, 1H), 9.19 (s, 1H), 8.25 (s, 1H), 8.09 (d, J = 8.2 Hz, 1H), 7.98 (s, 1H), 7.94 (d, J = 8.0 Hz, 1H), 7.87 (s, 1H), 7.79 (d, J = 8.8 Hz, 1H), 7.60 (t, J = 8.1 Hz, 1H), 7.54 (s, 1H), 7.52 (s, 1H), 7.46 (d, J = 7.5 Hz, 1H), 6.97 (s, 2H), 2.37 (s, 3H). ^{13}C NMR (126 MHz, DMSO-d_6) δ 165.88, 162.99, 161.53, 151.53, 140.98, 140.44, 139.97, 135.79, 134.33, 132.50, 131.19, 130.31, 129.79 (d, J = 31.4 Hz), 129.30, 128.30, 127.35, 124.90, 124.63 (d, J = 272.4 Hz), 124.26, 120.35 (d, J = 3.8 Hz), 119.74, 116.87 (d, J = 3.9 Hz), 20.79. HRMS m/z (ESI) found 423.1429 [M+H]$^+$, C$_{23}$H$_{18}$F$_3$N$_4$O$^+$ Calcd. for 423.1427, HPLC >99% pure.

4.2.11. General procedure B for syntheses of 16–24

To a solution of 6-bromo-2-chloroquinazoline (1 eq.) in isopropyl alcohol (10 mL) was added the corresponding amines (1.2 eq.), and N-ethyl-N,N-diisopropylamine (3 eq.). The reaction mixture was heated at 85 °C for 6 h. The reaction was cooled to room temperature, which was then brought to saturated salt solution and extracted with ethyl acetate. The organic layer was collected and distilled under reduced pressure. The crude residue was purified via by silica gel column chromatography to afford the intermediates 6-bromoquinazolines. The 6-bromoquinazolines reacted with 4-methyl-3-(4,4,5,5-tetramethyl-1,3,2-dioxaborolan-2-yl)-N-(3-(trifluoromethyl)phenyl) benzamide (m4) according to general procedure A to afford 16–24.

4.2.12. 3-(2-(Cyclopropylamino)quinazolin-6-yl)-4-methyl-N-(3-(trifluoromethyl)phenyl)benzamide (16)

Light green solid; yield: 71%. ^{1}H NMR (400 MHz, DMSO-d_6) δ 10.54 (s, 1H), 9.18 (s, 1H), 8.25 (s, 1H), 8.09 (d, J = 8.1 Hz, 1H), 7.98 (s, 1H), 7.94 (d, J = 8.2 Hz, 1H), 7.88 (s, 1H), 7.80 (d, J = 8.7 Hz, 1H), 7.71 (d, J = 3.4 Hz, 1H), 7.60 (t, J = 8.1 Hz, 2H), 7.52 (d, J = 8.0 Hz, 1H), 7.46 (d, J = 7.7 Hz, 1H), 2.98−2.81 (m, 1H), 2.37 (s, 3H), 0.75 (q, J = 6.0 Hz, 2H), 0.56 (q, J = 6.0, 5.0 Hz, 2H). ^{13}C NMR (126 MHz, DMSO-d_6) δ 165.89, 162.47, 161.26, 151.35, 140.95, 140.45, 139.96, 135.76, 134.43, 132.53, 131.20, 130.29, 129.80 (d, J = 31.5 Hz), 129.30, 128.37, 127.35, 125.31, 124.63 (d, J = 272.3 Hz), 124.26, 120.34

(d, J = 3.9 Hz), 120.06, 116.88 (d, J = 3.8 Hz), 24.52, 20.78, 6.87. HRMS m/z (ESI) found 463.1741 [M+H]$^+$, $C_{26}H_{22}F_3N_4O^+$ Calcd. for 463.174, HPLC >99% pure.

4.2.13. 4-Methyl-3-(2-((1-methylpiperidin-4-yl)amino) quinazolin-6-yl)-N-(3-(trifluoromethyl)phenyl)benzamide (17)

White solid; yield: 69%. ^{1}H NMR (400 MHz, DMSO-d_6) δ 10.54 (s, 1H), 9.17 (s, 1H), 8.25 (s, 1H), 8.09 (d, J = 8.4 Hz, 1H), 7.97 (s, 1H), 7.94 (d, J = 8.5 Hz, 1H), 7.86 (s, 1H), 7.77 (d, J = 8.5 Hz, 1H), 7.60 (t, J = 8.0 Hz, 1H), 7.54 (t, J = 9.4 Hz, 2H), 7.45 (t, J = 7.8 Hz, 2H), 3.94−3.77 (m, 1H), 2.80 (m, 2H), 2.37 (s, 3H), 2.21 (s, 3H), 2.04 (m, 2H), 1.93 (m, 2H), 1.58 (m, 2H). ^{13}C NMR (126 MHz, DMSO-d_6) δ 165.90, 162.71, 140.96, 140.44, 139.95, 135.77, 134.20, 132.52, 131.19, 130.30, 129.79 (d, J = 31.5 Hz), 129.29, 128.36, 127.32, 124.63 (d, J = 272.0 Hz), 124.26, 122.23, 120.34 (d, J = 3.9 Hz), 119.81, 116.87 (d, J = 3.8 Hz), 54.86, 46.43, 31.75, 29.45, 20.79. HRMS m/z (ESI) found 520.2332 [M+H]$^+$, $C_{29}H_{29}F_3N_5O^+$ Calcd. for 520.2319, HPLC >99% pure.

4.2.14. 4-Methyl-3-(2-((2-morpholinoethyl)amino)quinazolin-6-yl)-N-(3-(trifluoromethyl)phenyl)benzamide (18)

White solid; yield: 71%. ^{1}H NMR (400 MHz, chloroform-d) δ 8.95 (s, 1H), 8.43 (s, 1H), 7.97 (s, 1H), 7.91 (d, J = 8.1 Hz, 1H), 7.81 (d, J = 8.6 Hz, 2H), 7.62 (s, 2H), 7.54 (s, 1H), 7.45 (d, J = 7.9 Hz, 1H), 7.39 (t, J = 6.4 Hz, 2H), 5.93 (t, J = 4.4 Hz, 1H), 3.76−3.68 (m, 4H), 3.64 (q, J = 5.0 Hz, 2H), 2.64 (t, J = 5.8 Hz, 2H), 2.51 (m, 4H), 2.35 (s, 3H). ^{13}C NMR (126 MHz, chloroform-d) δ 165.10, 161.53, 159.22, 150.94, 140.87, 139.87, 138.14, 135.00, 134.37, 131.59, 130.95 (d, J = 32.7 Hz), 130.60, 129.12, 128.07, 126.98, 126.03 (d, J = 272.1 Hz), 125.75, 124.82, 122.74, 120.49 (d, J = 3.9 Hz), 119.38, 116.41 (d, J = 3.9 Hz), 66.50, 52.89, 37.32, 29.22, 20.15. HRMS m/z (ESI) found 536.2284 [M+H]$^+$, $C_{29}H_{29}F_3N_5O_2^+$ Calcd. for 536.2268, HPLC >99% pure.

4.2.15. 4-Methyl-3-(2-(4-methylpiperazin-1-yl)quinazolin-6-yl)-N-(3-(trifluoromethyl)phenyl)benzamide (19)

White solid; yield: 86%. ^{1}H NMR (400 MHz, DMSO-d_6) δ 10.54 (s, 1H), 9.27 (s, 1H), 8.25 (s, 1H), 8.09 (d, J = 8.2 Hz, 1H), 7.98 (s, 1H), 7.95 (d, J = 8.0 Hz, 1H), 7.90 (s, 1H), 7.82 (d, J = 8.6 Hz, 1H), 7.64−7.56 (m, 2H), 7.52 (d, J = 8.2 Hz, 1H), 7.45 (d, J = 7.5 Hz, 1H), 3.89 (s, 4H), 3.85 (d, J = 5.2 Hz, 1H), 3.38 (s, 1H), 2.51 (s, 2H), 2.36 (s, 3H), 2.24 (s, 3H). ^{13}C NMR (126 MHz, chloroform-d) δ 165.03, 160.99, 158.91, 151.14, 141.08, 139.97, 138.01, 134.85, 134.29, 131.56, 130.98 (d, J = 32.5 Hz), 130.61, 129.14, 128.04, 126.84, 126.04 (d, J = 217.1 Hz), 125.57, 125.09, 122.73, 120.55, 118.87, 116.40 (d, J = 4.1 Hz), 54.60, 45.78, 43.55, 20.18. HRMS m/z (ESI) found 506.2157 [M+H]$^+$, $C_{28}H_{27}F_3N_5O^+$ Calcd. for 506.2162, HPLC >99% pure.

4.2.16. 4-Methyl-3-(2-((4-(4-methylpiperazin-1-yl)phenyl) amino)quinazolin-6-yl)-N-(3-(trifluoromethyl)phenyl)benzamide (20)

Yellow solid; yield: 76%. ^{1}H NMR (400 MHz, DMSO-d_6) δ 10.54 (s, 1H), 9.73 (s, 1H), 9.30 (s, 1H), 8.24 (s, 1H), 8.08 (d, J = 9.1 Hz, 1H), 7.99 (s, 1H), 7.96 (s, 2H), 7.86 (dd, J = 8.6, 1.7 Hz, 1H), 7.82 (d, J = 8.8 Hz, 2H), 7.68 (d, J = 8.7 Hz, 1H), 7.60 (t, J = 7.9 Hz, 1H), 7.53 (d, J = 8.0 Hz, 1H), 7.45 (d, J = 8.0 Hz, 1H), 6.95 (d, J = 8.9 Hz, 2H), 3.19−3.03 (m, 4H), 2.52−2.50 (m, 4H) 2.38 (s, 3H), 2.26 (s, 3H). ^{13}C NMR (126 MHz, DMSO-d_6) δ 165.87, 162.61, 157.73, 150.70, 146.73, 140.83, 140.45, 139.97,

136.10, 135.33, 133.08, 132.56, 131.25, 130.32, 129.80 (d, J = 31.6 Hz), 129.34, 128.38, 127.46, 125.63, 124.63 (d, J = 272.4 Hz), 124.28, 120.60, 120.43, 116.90, 116.37, 55.08, 49.20, 46.08, 20.80. HRMS m/z (ESI) found 597.2596 [M+H]$^+$, $C_{34}H_{32}F_3N_6O^+$ Calcd. for 597.2584, HPLC >99% pure.

4.2.17. 4-Methyl-3-(2-((3-(4-methylpiperazin-1-yl)phenyl) amino)quinazolin-6-yl)-N-(3-(trifluoromethyl)phenyl)benzamide (21)

Yellow solid; yield: 76%. ^{1}H NMR (400 MHz, DMSO-d_6) δ 10.64 (s, 1H), 9.91 (s, 1H), 9.38 (s, 1H), 8.28 (s, 1H), 8.12 (d, J = 8.6 Hz, 1H), 8.02 (s, 2H), 7.99 (d, J = 8.4 Hz, 1H), 7.93 (d, J = 8.8 Hz, 1H), 7.90 (s, 1H), 7.78 (d, J = 8.8 Hz, 1H), 7.61 (t, J = 7.7 Hz, 1H), 7.55 (d, J = 8.0 Hz, 1H), 7.46 (d, J = 6.7 Hz, 2H), 7.23 (t, J = 8.0 Hz, 1H), 6.69 (d, J = 9.1 Hz, 1H), 3.81 (brs, 2H), 3.53 (brs, 2H), 3.20 (brs, 4H), 2.83 (s, 3H), 2.40 (s, 3H). ^{13}C NMR (126 MHz, DMSO-d_6) δ 165.89, 162.78, 157.55, 150.53, 150.32, 141.84, 140.74, 140.48, 139.98, 136.23, 135.96, 132.57, 131.25, 130.30, 129.78 (d, J = 31.6 Hz), 129.58, 129.45, 128.41, 127.54, 125.99, 124.30, 120.61, 120.37, 116.90, 111.46, 110.48, 107.03, 52.63, 46.23, 42.48, 20.90. HRMS m/z (ESI) found 597.2582 [M+H]$^+$, $C_{34}H_{32}F_3N_6O^+$ Calcd. for 597.2584, HPLC >99% pure.

4.2.18. 4-Methyl-3-(2-((1-methyl-1H-pyrazol-4-yl)amino) quinazolin-6-yl)-N-(3-(trifluoromethyl)phenyl)benzamide (22)

Yellow solid; yield: 82%. ^{1}H NMR (400 MHz, DMSO-d_6) δ 10.55 (s, 1H), 9.85 (s, 1H), 9.29 (s, 1H), 8.26 (s, 2H), 8.09 (d, J = 8.3 Hz, 1H), 8.00 (s, 1H), 7.96 (d, J = 7.3 Hz, 2H), 7.88 (d, J = 8.6 Hz, 1H), 7.77 (d, J = 7.7 Hz, 1H), 7.63 (d, J = 6.4 Hz, 1H), 7.60 (d, J = 8.2 Hz, 1H), 7.54 (d, J = 7.9 Hz, 1H), 7.46 (d, J = 7.8 Hz, 1H), 3.87 (s, 3H), 2.39 (s, 3H). ^{13}C NMR (126 MHz, DMSO-d_6) δ 165.88, 162.73, 157.14, 151.03, 140.86, 140.45, 139.97, 136.03, 135.16, 132.54, 131.23, 130.31, 129.80 (d, J = 31.5 Hz), 129.34, 128.40, 127.43, 125.71, 125.68, 124.63 (d, J = 272.1 Hz), 124.27, 123.66, 121.13, 120.35 (d, J = 3.8 Hz), 120.13, 116.88 (d, J = 3.8 Hz), 39.22, 20.79. HRMS m/z (ESI) found 503.1809 [M+H]$^+$, $C_{27}H_{22}F_3N_6O^+$ Calcd. for 503.1802, HPLC >99% pure.

4.2.19. 3-(4-Amino-2-((1-methyl-1H-pyrazol-4-yl)amino) quinazolin-6-yl)-4-methyl-N-(3-(trifluoromethyl)phenyl) benzamide (23)

Yellow solid; yield: 72%. ^{1}H NMR (400 MHz, DMSO-d_6) δ 10.55 (s, 1H), 8.90 (s, 1H), 8.26 (s, 1H), 8.11 (s, 2H), 8.09 (s, 1H), 7.99 (s, 1H), 7.93 (d, J = 8.0 Hz, 1H), 7.65 (d, J = 8.7 Hz, 1H), 7.61 (t, J = 8.1 Hz, 1H), 7.54 (s, 1H), 7.52 (d, J = 8.1 Hz, 1H), 7.46 (d, J = 8.0 Hz, 2H), 3.82 (s, 3H), 2.40 (s, 3H). ^{13}C NMR (126 MHz, DMSO-d_6) δ 165.98, 162.67, 157.51, 151.79, 141.55, 140.47, 140.01, 134.14, 133.18, 132.41, 131.08, 130.31, 130.13, 129.79 (d, J = 31.6 Hz), 129.44, 127.07, 125.34, 124.66, 124.63 (d, J = 272.3 Hz), 124.44, 124.24, 120.77, 120.31, 116.84 (d, J = 3.9 Hz), 39.11, 20.88. HRMS m/z (ESI) found 518.1912 [M+H]$^+$, $C_{27}H_{23}F_3N_7O^+$ Calcd. for 518.1911, HPLC >99% pure.

4.2.20. 3-(2-((1-Cyclopropyl-1H-pyrazol-4-yl)amino) quinazolin-6-yl)-4-methyl-N-(3-(trifluoromethyl)phenyl) benzamide (24)

Yellow solid; yield: 79%. ^{1}H NMR (400 MHz, DMSO-d_6) δ 10.55 (s, 1H), 9.85 (s, 1H), 9.29 (s, 1H), 8.25 (s, 1H), 8.09 (d, J = 8.3 Hz, 1H), 8.00 (d, J = 2.0 Hz, 1H), 7.98−7.92 (m, 2H), 7.88 (dd, J = 8.6, 2.0 Hz, 1H), 7.78 (d, J = 8.7 Hz, 1H), 7.65−7.57 (m, 2H), 7.54 (d, J = 8.0 Hz, 1H), 7.46 (d, J = 7.8 Hz, 1H), 3.75

(tt, J = 7.4, 3.9 Hz, 1H), 2.39 (s, 3H), 1.11−1.02 (m, 2H), 1.01−0.94 (m, 2H). ^{13}C NMR (126 MHz, DMSO-d_6) δ 165.90, 162.78, 151.00, 140.88, 140.46, 139.99, 136.06, 135.24, 132.56, 131.25, 130.49, 130.33, 129.35, 128.40, 127.45, 125.75, 124.28, 123.50, 120.38, 120.32, 120.17, 116.91, 116.88, 33.16, 20.80, 6.63. HRMS m/z (ESI) found 529.197 [M+H]$^+$, $C_{29}H_{24}F_3N_6O^+$ Calcd. for 529.1958, HPLC >99% pure.

4.2.21. General procedure C for the preparation of compounds 25–31

M11 (300 mg, 0.6 mmol) and triethylamine (122 mg, 1.2 mmol) was dissolved in 15 mL DCM. The mixture was added corresponding amines and stirred at room temperature for 6 h (piperazine derivatives for **25–29** and **31** and homopiperazine for **30**). The mixture was then brought to saturated salt solution and extracted with DCM for 3 times. The organic layer was collected, dried with Na_2SO_4 and distilled under reduced pressure. The crude residue was purified via by silica gel column chromatography to afford the intermediate **m12**. 6-Bromo-N-(1-methyl-1H-pyrazol-4-yl)quinazolin-2-amine reacted with **m12** according to general procedure B to get **25–31**.

4.2.22. 4-Methyl-3-(2-((1-methyl-1H-pyrazol-4-yl)amino)quinazolin-6-yl)-N-(3-((4-methylpiperazin-1-yl)methyl)-5-(trifluoromethyl)phenyl)benzamide (25)

Yellow solid; yield 73%. ^{1}H NMR (400 MHz, DMSO-d_6) δ 10.54 (s, 1H), 9.85 (s, 1H), 9.29 (s, 1H), 8.24 (s, 1H), 8.20 (s, 1H), 8.04 (s, 1H), 8.02 (s, 1H), 7.96 (d, J = 7.9 Hz, 2H), 7.88 (d, J = 8.9 Hz, 1H), 7.76 (d, J = 7.8 Hz, 1H), 7.64 (s, 1H), 7.54 (d, J = 8.1 Hz, 1H), 7.37 (s, 1H), 3.87 (s, 3H), 3.56 (s, 2H), 2.64−2.53 (m, 4H), 2.50−2.42 (m, 4H), 2.39 (s, 3H), 2.29 (s, 3H). ^{13}C NMR (126 MHz, DMSO-d_6) δ 165.83, 162.72, 151.01, 140.92, 140.83, 140.49, 139.97, 136.03, 135.16, 132.48, 131.23, 130.30, 130.09, 129.68 (d, J = 31.4 Hz), 129.33, 128.40, 127.45, 125.67, 124.65 (d, J = 272.2 Hz), 124.37, 123.65, 121.12, 120.44, 120.12, 115.66, 61.65, 54.65, 52.22, 45.31, 39.22, 20.80. HRMS m/z (ESI) found 615.2813 [M+H]$^+$, $C_{33}H_{34}F_3N_8O^+$ Calcd. for 615.2802, HPLC >99% pure.

4.2.23. N-(3-((4-Isopropylpiperazin-1-yl)methyl)-5-(trifluoromethyl)phenyl)-4-methyl-3-(2-((1-methyl-1H-pyrazol-4-yl)amino)quinazolin-6-yl)benzamide (26)

Yellow solid; yield 76%. ^{1}H NMR (400 MHz, DMSO-d_6) δ 10.52 (s, 1H), 9.84 (s, 1H), 9.29 (s, 1H), 8.23 (d, J = 13.1 Hz, 2H), 8.01 (s, 2H), 7.96 (d, J = 7.3 Hz, 2H), 7.88 (d, J = 9.3 Hz, 1H), 7.76 (d, J = 8.0 Hz, 1H), 7.64 (s, 1H), 7.54 (d, J = 8.4 Hz, 1H), 7.35 (s, 1H), 3.87 (s, 3H), 3.53 (s, 2H), 2.66−2.54 (m, 2H), 2.47−2.28 (m, 10H), 0.95 (d, J = 6.4 Hz, 6H). ^{13}C NMR (126 MHz, DMSO-d_6) δ 165.83, 162.72, 157.05, 151.02, 141.21, 140.82, 140.46, 139.95, 136.03, 135.17, 132.51, 131.22, 130.30, 129.62 (d, J = 31.5 Hz), 129.33, 128.39, 127.45, 125.66, 124.67 (d, J = 272.2 Hz), 124.27, 123.65, 121.12, 120.39, 120.12, 115.55, 62.01, 54.02, 53.54, 48.40, 39.22, 20.80, 18.72. HRMS m/z (ESI) found 643.3122 [M+H]$^+$, $C_{35}H_{38}F_3N_8O^+$ Calcd. for 643.3115, HPLC >99% pure.

4.2.24. N-(3-((4-Cyclopentylpiperazin-1-yl)methyl)-5-(trifluoromethyl)phenyl)-4-methyl-3-(2-((1-methyl-1H-pyrazol-4-yl)amino)quinazolin-6-yl)benzamide (27)

Yellow solid; yield 71%. ^{1}H NMR (400 MHz, DMSO-d_6) δ 10.52 (s, 1H), 9.85 (s, 1H), 9.28 (s, 1H), 8.23 (d, J = 14.2 Hz, 2H), 8.02 (s, 2H), 7.95 (d, J = 7.9 Hz, 2H), 7.88 (d, J = 8.9 Hz, 1H), 7.76 (d, J = 7.5 Hz, 1H), 7.64 (s, 1H), 7.53 (d, J = 8.0 Hz, 1H), 7.34 (s, 1H), 3.87 (s, 3H), 3.52 (s, 2H), 2.52 (s, 4H), 2.47−2.31 (m, 8H), 1.81−1.68 (m, 2H), 1.64−1.53 (m, 2H), 1.51−1.38 (m, 2H), 1.35−1.21 (m, 2H). ^{13}C NMR (126 MHz, DMSO-d_6) δ 165.83, 162.73, 157.09, 151.04, 141.14, 140.83, 140.47, 139.95, 136.04, 135.17, 132.51, 131.23, 130.32, 129.64 (d, J = 31.0 Hz), 129.33, 128.40, 127.46, 125.68, 124.67 (d, J = 272.0 Hz), 124.28, 123.66, 121.13, 120.41, 120.13, 115.56, 67.18, 61.96, 53.21, 52.08, 39.22, 30.37, 24.09, 20.79. HRMS m/z (ESI) found 669.3272 [M+H]$^+$, $C_{37}H_{40}F_3N_8O^+$ Calcd. for 669.3272, HPLC >99% pure.

4.2.25. N-(3-((4-Acetylpiperazin-1-yl)methyl)-5-(trifluoromethyl)phenyl)-4-methyl-3-(2-((1-methyl-1H-pyrazol-4-yl)amino)quinazolin-6-yl)benzamide (28)

Yellow solid; yield 65%. ^{1}H NMR (400 MHz, DMSO-d_6) δ 10.54 (s, 1H), 9.85 (s, 1H), 9.29 (s, 1H), 8.23 (d, J = 11.3 Hz, 2H), 8.05 (s, 1H), 8.02 (s, 1H), 7.96 (d, J = 8.8 Hz, 2H), 7.88 (d, J = 7.7 Hz, 1H), 7.77 (d, J = 7.7 Hz, 1H), 7.64 (s, 1H), 7.54 (d, J = 8.0 Hz, 1H), 7.38 (s, 1H), 3.87 (s, 3H), 3.58 (s, 2H), 3.49−3.39 (m, 4H), 2.39 (s, 3H), 2.36−2.31 (m, 4H), 1.98 (s, 3H). ^{13}C NMR (126 MHz, DMSO-d_6) δ 168.57, 165.84, 162.74, 157.14, 151.03, 140.84, 140.75, 140.52, 139.99, 136.05, 135.17, 132.49, 131.25, 130.32, 129.71 (d, J = 31.8 Hz), 129.33, 128.40, 127.46, 125.68, 124.65 (d, J = 272.3 Hz), 124.40, 123.66, 121.14, 120.54, 120.13, 115.72, 61.72, 53.21, 46.09, 39.22, 21.63, 20.79. HRMS m/z (ESI) found 643.2746 [M+H]$^+$, $C_{34}H_{34}F_3N_8O_2^+$ Calcd. for 643.2751, HPLC >99% pure.

4.2.26. N-(3-((3,5-Dimethylpiperazin-1-yl)methyl)-5-(trifluoromethyl)phenyl)-4-methyl-3-(2-((1-methyl-1H-pyrazol-4-yl)amino)quinazolin-6-yl)benzamide (29)

Yellow solid; yield 63%. ^{1}H NMR (400 MHz, DMSO-d_6) δ 10.52 (s, 1H), 9.85 (s, 1H), 9.29 (s, 1H), 8.22 (d, J = 12.5 Hz, 2H), 8.02 (s, 2H), 7.96 (d, J = 8.0 Hz, 2H), 7.88 (d, J = 8.9 Hz, 1H), 7.77 (d, J = 8.1 Hz, 1H), 7.64 (s, 1H), 7.54 (d, J = 8.1 Hz, 1H), 7.35 (s, 1H), 3.87 (s, 3H), 3.54 (s, 2H), 2.48−2.24 (m, 10H), 0.98 (t, J = 7.1 Hz, 6H). ^{13}C NMR (126 MHz, DMSO-d_6) δ 165.83, 162.72, 157.03, 151.02, 141.17, 140.82, 140.47, 139.95, 136.03, 135.17, 132.50, 131.23, 130.31, 129.64 (d, J = 30.9 Hz), 129.33, 128.39, 127.45, 125.67, 124.67 (d, J = 272.1 Hz), 124.29, 123.65, 121.12, 120.39, 120.12, 115.56, 61.93, 53.10, 52.77, 39.22, 20.79, 12.45. HRMS m/z (ESI) found 629.2965 [M+H]$^+$, $C_{34}H_{36}F_3N_8O^+$ Calcd. for 629.2959, HPLC >99% pure.

4.2.27. 4-Methyl-N-(3-((4-methyl-1,4-diazepan-1-yl)methyl)-5-(trifluoromethyl)phenyl)-3-(2-((1-methyl-1H-pyrazol-4-yl)amino)quinazolin-6-yl)benzamide (30)

Yellow solid; yield 74%. ^{1}H NMR (400 MHz, DMSO-d_6) δ 10.54 (s, 1H), 9.85 (s, 1H), 9.29 (s, 1H), 8.24 (s, 1H), 8.18 (s, 1H), 8.07 (s, 1H), 8.01 (s, 1H), 7.96 (d, J = 6.8 Hz, 2H), 7.88 (d, J = 8.9 Hz, 1H), 7.77 (d, J = 10.6 Hz, 1H), 7.64 (s, 1H), 7.54 (d, J = 8.2 Hz, 1H), 7.39 (s, 1H), 3.87 (s, 3H), 3.71 (s, 2H), 2.77−2.64 (m, 8H), 2.39 (s, 6H), 1.85−1.70 (m, 2H). ^{13}C NMR (126 MHz, DMSO-d_6) δ 165.84, 162.72, 157.06, 151.02, 142.22, 140.83, 140.47, 139.95, 136.03, 135.16, 132.53, 131.23, 130.31, 129.66 (d, J = 31.6 Hz), 129.34, 128.40, 127.45, 125.68, 124.68 (d, J = 272.2 Hz), 124.08, 123.63 (d, J = 5.3 Hz), 121.13, 120.12, 115.52, 61.55, 57.35, 56.32, 54.10, 46.28, 39.23, 20.80. HRMS m/z (ESI) found 629.2958 [M+H]$^+$, $C_{34}H_{36}F_3N_8O^+$ Calcd. for 629.2959, HPLC >99% pure.

4.2.28. 4-Methyl-3-(2-((1-methyl-1H-pyrazol-4-yl)amino) quinazolin-6-yl)-N-(3-(((1R,5S)-8-methyl-3,8-diazabicyclo[3.2.1] octan-3-yl)methyl)-5-(trifluoromethyl)phenyl)benzamide (31)
Yellow solid; yield 63%. ^{1}H NMR (400 MHz, DMSO-d_6) δ 10.53 (s, 1H), 9.85 (s, 1H), 9.29 (s, 1H), 8.25 (s, 1H), 8.18 (s, 1H), 8.09 (s, 1H), 8.01 (s, 1H), 7.96 (d, J = 6.6 Hz, 2H), 7.88 (dd, J = 8.6, 1.9 Hz, 1H), 7.77 (d, J = 7.1 Hz, 1H), 7.64 (s, 1H), 7.54 (d, J = 8.2 Hz, 1H), 7.42 (s, 1H), 3.87 (s, 3H), 3.55 (s, 2H), 3.18 (d, J = 5.3 Hz, 2H), 3.05 (s, 2H), 2.39 (s, 3H), 2.18 (d, J = 10.3 Hz, 2H), 2.13 (s, 2H), 1.94−1.85 (m, 2H), 1.71 (d, J = 6.7 Hz, 2H). ^{13}C NMR (126 MHz, DMSO-d_6) δ 165.85, 162.72, 151.02, 142.74, 140.82, 140.39, 139.92, 136.04, 135.17, 132.59, 131.21, 130.29, 129.56 (d, J = 32.2 Hz), 129.34, 128.40, 127.45, 125.80, 125.67, 124.07, 123.65, 121.13, 120.12, 115.40, 61.25, 59.46, 56.04, 45.46, 39.51, 26.42, 20.80. HRMS m/z (ESI) found 641.2967 [M+H]$^+$, C$_{35}$H$_{36}$F$_3$N$_8$O$^+$ Calcd. for 641.2959, HPLC >99% pure.

4.2.29. General procedure D for the preparation of compounds 32–36
4-Substituted-3-bromobenzoic acids (**m13**, 1 eq.) was dissolved in dimethyl formamide. The solution was added HATU (1.1 eq.), DIEA (2.0 eq.) and 3-(trifluoromethyl) aniline (1.0 eq.), and then stirred for about 12 h at room temperature. The reaction mixture was diluted with ethyl acetate, and washed with a saturated aqueous sodium bicarbonate solution and saline. The organic layer thus obtained was dried over anhydrous sodium sulfate, filtered, and concentrated under reduced pressure. The crude product was purified by column chromatography to give intermediate **m14**. An oven-dried Schlenk flask in a glove box was charged with **m14** (1 eq.), bis(pinacolato) diboron (1.5 eq.), PdCl$_2$(dppf)·CH$_2$Cl$_2$ (5 mol %), and KOAc (3.0 eq.). The flask was sealed with a septum, removed from the glove box, and purged with Ar. DMSO was added and the mixture was heated to 80 °C for 8 h under Ar then cooled to rt. The mixture was then filtered through diatomite, which was subsequently washed with EtOAc (100 mL). The filtrate was washed successively with H$_2$O and brine, then dried with Na$_2$SO$_4$ and concentrated. The crude product was purified by column chromatography to get intermediate **m15**. 6-Bromo-N-(1-methyl-1H-pyrazol-4-yl)quinazolin-2-amine (for **32–35**) or 6-bromo-N-(1-cyclopropyl-1H-pyrazol-4-yl)quinazolin-2-amine (for **36**) reacted with **m15** according to general procedure B to get **32–36**.

4.2.30. 4-Ethyl-3-(2-((1-methyl-1H-pyrazol-4-yl)amino) quinazolin-6-yl)-N-(3-(trifluoromethyl)phenyl)benzamide (32)
Yellow solid; yield 78%. ^{1}H NMR (400 MHz, DMSO-d_6) δ 10.54 (s, 1H), 9.85 (s, 1H), 9.29 (s, 1H), 8.25 (s, 2H), 8.09 (d, J = 8.9 Hz, 1H), 7.99 (d, J = 8.0 Hz, 1H), 7.96 (s, 1H), 7.91 (s, 1H), 7.83 (d, J = 8.5 Hz, 1H), 7.77 (d, J = 8.6 Hz, 1H), 7.63 (d, J = 5.5 Hz, 1H), 7.62−7.56 (m, 2H), 7.46 (d, J = 8.4 Hz, 1H), 3.87 (s, 3H), 2.70 (q, J = 7.6 Hz, 2H), 1.11 (t, J = 7.5 Hz, 3H). ^{13}C NMR (126 MHz, DMSO-d_6) δ 165.89, 162.73, 151.02, 146.00, 140.65, 140.45, 136.01, 135.21, 132.35, 130.32, 129.80 (d, J = 31.5 Hz), 129.53, 128.27, 127.76, 125.71, 124.65 (d, J = 272.3 Hz), 124.26, 123.66, 121.12, 120.36 (d, J = 3.8 Hz), 120.10, 116.86 (d, J = 3.8 Hz), 39.23, 26.20, 15.65.HRMS m/z (ESI) found 517.1964 [M+H]$^+$, C$_{28}$H$_{24}$F$_3$N$_6$O$^+$ Calcd. for 517.1958, HPLC >99% pure.

4.2.31. 4-Methoxy-3-(2-((1-methyl-1H-pyrazol-4-yl)amino) quinazolin-6-yl)-N-(3-(trifluoromethyl)phenyl)benzamide (33)
Yellow solid; yield 70%. ^{1}H NMR (400 MHz, DMSO-d_6) δ 10.48 (s, 1H), 9.83 (s, 1H), 9.28 (s, 1H), 8.29−8.20 (m, 2H), 8.11 (s, 1H), 8.08 (s, 1H), 8.06 (s, 1H), 8.00 (d, J = 8.8 Hz, 1H), 7.73 (d, J = 10.2 Hz,

1H), 7.63 (s, 1H), 7.60 (d, J = 8.1 Hz, 1H), 7.46 (d, J = 7.9 Hz, 1H), 7.34 (d, J = 8.7 Hz, 1H), 3.92 (s, 3H), 3.87 (s, 3H). ^{13}C NMR (126 MHz, DMSO-d_6) δ 165.57, 162.72, 159.58, 157.09, 151.09, 140.58, 136.37, 132.22, 130.46, 130.30, 129.82, 129.79 (d, J = 31.6 Hz), 129.03, 128.53, 127.07, 125.29, 124.66 (d, J = 272.1 Hz), 124.22, 123.68, 121.11, 120.23, 120.16 (d, J = 3.8 Hz), 116.83 (d, J = 3.8 Hz), 112.11, 56.54, 39.23. HRMS m/z (ESI) found 519.1759 [M+H]$^+$, C$_{27}$H$_{22}$F$_3$N$_6$O$_2^+$ Calcd. for 519.1751, HPLC >99% pure.

4.2.32. 4-Isopropyl-3-(2-((1-methyl-1H-pyrazol-4-yl)amino) quinazolin-6-yl)-N-(3-(trifluoromethyl)phenyl)benzamide (34)
Yellow solid; yield 72%. ^{1}H NMR (400 MHz, DMSO-d_6) δ 10.53 (s, 1H), 9.85 (s, 1H), 9.30 (s, 1H), 8.25 (s, 2H), 8.08 (d, J = 8.0 Hz, 1H), 8.03 (d, J = 8.9 Hz, 1H), 7.92 (s, 1H), 7.88 (s, 1H), 7.78 (s, 2H), 7.67 (d, J = 8.5 Hz, 1H), 7.63 (d, J = 9.9 Hz, 1H), 7.59 (d, J = 8.0 Hz, 1H), 7.46 (d, J = 7.6 Hz, 1H), 3.87 (s, 3H), 3.10 (p, J = 7.1 Hz, 1H), 1.20 (d, J = 6.7 Hz, 6H). ^{13}C NMR (126 MHz, DMSO-d_6) δ 165.91, 162.72, 157.10, 151.01, 150.68, 140.45, 140.13, 136.11, 135.32, 132.10, 130.31, 129.80 (d, J = 31.6 Hz), 129.52, 128.29, 128.01, 126.56, 125.71, 125.66, 124.23, 123.67, 124.75 (d, J = 272.1 Hz), 121.11, 120.34 (d, J = 3.8 Hz), 120.08, 116.84 (d, J = 3.8 Hz), 39.23, 29.81, 24.21. HRMS m/z (ESI) found 531.2109 [M+H]$^+$, C$_{29}$H$_{26}$F$_3$N$_6$O$^+$ Calcd. for 531.2115, HPLC >99% pure.

4.2.33. 4-Cyclopropyl-3-(2-((1-methyl-1H-pyrazol-4-yl)amino) quinazolin-6-yl)-N-(3-(trifluoromethyl)phenyl)benzamide (35)
Yellow solid; yield 65%. ^{1}H NMR (400 MHz, DMSO-d_6) δ 10.53 (s, 1H), 9.85 (s, 1H), 9.31 (s, 1H), 8.25 (s, 2H), 8.08 (d, J = 8.5 Hz, 1H), 8.00 (d, J = 7.6 Hz, 2H), 7.98−7.89 (m, 2H), 7.78 (d, J = 10.3 Hz, 1H), 7.63 (d, J = 7.5 Hz, 1H), 7.59 (d, J = 8.2 Hz, 1H), 7.46 (d, J = 7.8 Hz, 1H), 7.19 (d, J = 8.3 Hz, 1H), 3.87 (s, 3H), 1.95 (td, J = 8.6, 4.6 Hz, 1H), 0.97 (q, J = 5.1, 3.8 Hz, 2H), 0.84 (q, J = 5.1 Hz, 2H). ^{13}C NMR (126 MHz, DMSO-d_6) δ 165.82, 162.76, 157.02, 151.03, 145.57, 141.13, 140.46, 136.37, 135.17, 131.71, 130.30, 129.79 (d, J = 31.5 Hz), 129.18, 128.62, 127.84, 125.61, 124.64 (d, J = 272.1 Hz), 124.56, 124.25, 123.67, 121.11, 120.35 (d, J = 3.8 Hz), 120.14, 116.86 (d, J = 4.0 Hz), 39.23, 14.12, 10.83. HRMS m/z (ESI) found 529.1970 [M+H]$^+$, C$_{29}$H$_{24}$F$_3$N$_6$O$^+$ Calcd. for 529.1958, HPLC >99% pure.

4.2.34. 4-Cyclopropyl-3-(2-((1-cyclopropyl-1H-pyrazol-4-yl) amino)quinazolin-6-yl)-N-(3-(trifluoromethyl)phenyl)benzamide (36)
Yellow solid; yield 60%. ^{1}H NMR (400 MHz, DMSO-d_6) δ 10.53 (s, 1H), 9.84 (s, 1H), 9.31 (s, 1H), 8.25 (s, 1H), 8.09 (d, J = 8.3 Hz, 1H), 8.03−7.98 (m, 2H), 7.98−7.90 (m, 2H), 7.79 (d, J = 9.4 Hz, 1H), 7.64 (s, 1H), 7.60 (t, J = 8.0 Hz, 1H), 7.45 (d, J = 7.8 Hz, 1H), 7.18 (d, J = 8.4 Hz, 1H), 3.74 (td, J = 7.2, 3.8 Hz, 1H), 1.94 (p, J = 8.0, 3.9 Hz, 1H), 1.08 (s, 2H), 1.02−0.95 (m, 4H), 0.84 (d, J = 5.3 Hz, 2H). ^{13}C NMR (126 MHz, DMSO-d_6) δ 165.84, 162.80, 157.08, 151.00, 145.58, 141.14, 140.48, 136.40, 135.25, 131.73, 130.48, 130.31, 129.19, 128.61, 127.86, 125.71, 124.57, 124.26, 123.52, 120.31, 120.18, 116.89, 33.16, 14.12, 10.83, 6.63. HRMS m/z (ESI) found 555.2115 [M+H]$^+$, C$_{31}$H$_{26}$F$_3$N$_6$O$^+$ Calcd. for 555.2115, HPLC >99% pure.

4.2.35. 1-(4-Methyl-3-(2-((1-methyl-1H-pyrazol-4-yl)amino) quinazolin-6-yl)phenyl)-3-(3-(trifluoromethyl)phenyl)urea (37)
6-Bromo-N-(1-methyl-1H-pyrazol-4-yl)quinazolin-2-amine reacted with **m18** according to general procedure B to get **37** as yellow solid; yield 78%. ^{1}H NMR (400 MHz, DMSO-d_6) δ 9.82 (s, 1H),

9.28 (s, 1H), 9.07 (s, 1H), 8.83 (s, 1H), 8.24 (s, 1H), 8.04 (s, 1H), 7.85 (s, 1H), 7.79 (dd, J = 8.7, 1.6 Hz, 1H), 7.72 (d, J = 8.5 Hz, 1H), 7.63 (s, 1H), 7.57 (d, J = 8.5 Hz, 1H), 7.53 (s, 1H), 7.50 (d, J = 7.8 Hz, 1H), 7.34 (d, J = 8.4 Hz, 1H), 7.31 (d, J = 7.5 Hz, 1H), 7.26 (d, J = 8.3 Hz, 1H), 3.87 (s, 3H), 2.24 (s, 3H). ^{13}C NMR (126 MHz, DMSO-d_6) δ 162.71, 157.09, 153.03, 150.85, 141.08, 137.80, 136.08, 135.99, 131.30, 130.34, 130.28, 129.98 (d, J = 31.4 Hz), 129.06, 127.95, 125.55, 124.68 (d, J = 272.2 Hz), 123.72, 122.29, 121.08, 120.27, 120.12, 118.48 (d, J = 3.8 Hz), 118.27, 114.56 (d, J = 3.8 Hz), 39.21, 20.00. HRMS m/z (ESI) found 518.1921 [M+H]$^+$, C$_{27}$H$_{23}$F$_3$N$_7$O$^+$ Calcd. for 518.1911, HPLC >99% pure.

4.2.36. 4-Methyl-3-(2-((1-methyl-1H-pyrazol-4-yl)amino) quinazolin-6-yl)-N-(3-(trifluoromethyl)benzyl)benzamide (38)

38 was prepared according to general procedure B as yellow solid; yield 73%. ^{1}H NMR (400 MHz, DMSO-d_6) δ 9.82 (s, 1H), 9.26 (s, 1H), 9.19 (t, J = 5.9 Hz, 1H), 8.23 (s, 1H), 7.90 (d, J = 1.9 Hz, 1H), 7.88 (d, J = 1.6 Hz, 1H), 7.87−7.85 (m, 1H), 7.85−7.81 (m, 1H), 7.74 (d, J = 8.9 Hz, 1H), 7.68 (s, 1H), 7.63 (t, J = 8.0 Hz, 3H), 7.60−7.55 (m, 1H), 7.47 (d, J = 7.9 Hz, 1H), 4.57 (d, J = 5.8 Hz, 2H), 3.86 (s, 3H), 2.35 (s, 3H). ^{13}C NMR (126 MHz, DMSO-d_6) δ 165.98, 162.24, 150.50, 141.25, 140.31, 138.80, 135.57, 134.84, 131.86, 131.50, 130.66, 129.82, 129.41, 128.98 (d, J = 31.4 Hz), 128.50, 126.45, 125.16, 124.32 (d, J = 272.5 Hz), 123.85 (t, J = 3.8 Hz), 123.54 (d, J = 4.1 Hz), 123.19, 120.66, 119.64, 42.30, 38.76, 20.25. HRMS m/z (ESI) found 517.1948 [M+H]$^+$, C$_{28}$H$_{24}$F$_3$N$_6$O$^+$ Calcd. for 517.1958, HPLC >99% pure.

4.2.37. N-(4-Methyl-3-(2-((1-methyl-1H-pyrazol-4-yl)amino) quinazolin-6-yl)phenyl)-2-(3-(trifluoromethyl)phenyl) propanamide (39)

39 was synthesized according to general procedure D as yellow solid; yield 76%. ^{1}H NMR (400 MHz, DMSO-d_6) δ 10.21 (s, 1H), 9.81 (s, 1H), 9.25 (s, 1H), 8.22 (s, 1H), 7.82 (s, 1H), 7.75 (d, J = 10.7 Hz, 2H), 7.70 (d, J = 7.2 Hz, 2H), 7.63 (d, J = 7.9 Hz, 2H), 7.60 (d, J = 7.4 Hz, 2H), 7.49 (d, J = 1.8 Hz, 1H), 7.26 (d, J = 8.4 Hz, 1H), 3.96 (q, J = 7.5 Hz, 1H), 3.86 (s, 3H), 2.22 (s, 3H), 1.46 (d, J = 6.9 Hz, 3H). ^{13}C NMR (126 MHz, DMSO-d_6) δ 171.98, 162.68, 150.81, 143.57, 140.98, 137.52, 135.88, 131.96, 131.23, 130.29, 129.98, 129.51 (d, J = 31.5 Hz), 127.92, 125.53, 124.71 (d, J = 272.2 Hz), 124.34, 124.05, 123.67, 121.09, 120.94, 120.09, 118.78, 46.19, 39.21, 20.06, 19.13. HRMS m/z (ESI) found 531.2123 [M+H]$^+$, C$_{29}$H$_{26}$F$_3$N$_6$O$^+$ Calcd. for 531.2115, HPLC >99% pure.

4.2.38. N-(1-(4-Methyl-3-(2-((1-methyl-1H-pyrazol-4-yl)amino) quinazolin-7-yl)phenyl)ethyl)-3-(trifluoromethyl)benzamide (40)

1-(3-Bromo-4-methylphenyl)ethan-1-one (5 g, 23.47 mmol) was dissolved in 100 mL methanol, followed by the addition of 4 Å molecular sieve (2 g) and ammonium acetate (18 g, 234.7 mmol). After stirred for 2 h at room temperature, the mixture was cooled to 0 °C and added sodium cyanoborohydride (4.42 g, 70.4 mmol) gradually. After the mixture was stirred for another 48 h, the solvent was removed under vacuum. The residue was added EtOAc and was washed with water. The organic layer was collected, dried with Na$_2$SO$_4$ and distilled under reduced pressure. The crude residue was dispersed in HCl in ether and white precipitate was formed. The white solid was filtered and washed with ether to get **m23** 4.8 g; yield 81.7%. The synthesis methods from **m23** to **40** was carried according to general procedure D. Yellow solid, yield 60% (three steps). ^{1}H NMR (400 MHz, DMSO-d_6) δ 9.79 (s, 1H), 9.25 (s, 1H),

9.10 (d, J = 8.0 Hz, 1H), 8.23 (s, 1H), 8.19 (d, J = 7.9 Hz, 1H), 7.91 (d, J = 7.4 Hz, 1H), 7.84 (d, J = 1.9 Hz, 1H), 7.78 (dd, J = 8.6, 2.0 Hz, 1H), 7.72 (t, J = 7.9 Hz, 2H), 7.62 (s, 1H), 7.35 (s, 1H), 7.34 (d, J = 1.7 Hz, 1H), 7.30 (d, J = 8.5 Hz, 1H), 5.23 (p, J = 7.8 Hz, 1H), 3.86 (s, 3H), 2.27 (s, 3H), 1.54 (d, J = 7.0 Hz, 3H). ^{13}C NMR (126 MHz, DMSO-d_6) δ 164.48, 162.67, 157.04, 150.83, 142.83, 140.68, 136.10, 135.83, 133.84, 132.04, 130.94, 130.28, 130.07, 129.54 (d, J = 32.0 Hz), 128.26, 128.23, 128.03, 125.78, 125.56, 125.53, 124.49 (d, J = 272.4 Hz), 124.35 (d, J = 4.2 Hz), 123.71, 123.39, 121.08, 120.12, 48.96, 39.22, 22.67, 20.30. HRMS m/z (ESI) found 531.2118 [M+H]$^+$, C$_{29}$H$_{26}$F$_3$N$_6$O$^+$ Calcd. for 531.2115, HPLC >99% pure.

4.2.39. N-(1-(4-Ethyl-3-(2-((1-methyl-1H-pyrazol-4-yl)amino) quinazolin-7-yl)phenyl)ethyl)-3-(trifluoromethyl)benzamide (41)

41 was prepared using the same method as **40** with 1-(3-bromo-4-ethylphenyl)ethan-1-one as the starting material. Yellow solid; yield 55%. ^{1}H NMR (400 MHz, DMSO-d_6) δ 9.80 (s, 1H), 9.25 (s, 1H), 9.10 (d, J = 7.9 Hz, 1H), 8.23 (s, 1H), 8.21 (s, 1H), 8.19 (s, 1H), 7.91 (d, J = 7.9 Hz, 1H), 7.80 (s, 1H), 7.76−7.67 (m, 3H), 7.62 (s, 1H), 7.39 (dd, J = 8.0, 1.7 Hz, 1H), 7.34 (d, J = 8.0 Hz, 1H), 7.30 (s, 1H), 5.23 (p, J = 7.2 Hz, 1H), 3.86 (s, 3H), 2.58 (q, J = 7.6 Hz, 2H), 1.53 (d, J = 7.0 Hz, 3H), 1.04 (t, J = 7.5 Hz, 3H). ^{13}C NMR (126 MHz, DMSO-d_6) δ 163.98, 162.20, 156.46, 150.34, 142.12, 139.99, 139.64, 135.68, 135.62, 135.31, 131.58, 129.60, 129.07 (d, J = 32.0 Hz), 128.76, 127.72, 127.46, 126.70 (d, J = 272.5 Hz), 125.08, 123.90 (d, J = 4.1 Hz), 123.24, 122.93, 120.59, 119.61, 48.45, 38.76, 25.33, 22.19, 15.52. HRMS m/z (ESI) found 545.228 [M+H]$^+$, C$_{30}$H$_{28}$F$_3$N$_6$O$^+$ Calcd. for 545.2271, HPLC >99% pure.

4.2.40. N-(1-(4-Methyl-3-(2-((1-methyl-1H-pyrazol-4-yl)amino) quinazolin-7-yl)phenyl)propyl)-3-(trifluoromethyl)benzamide (42)

142 was prepared using the same method as **40** with 1-(3-bromo-4-methylphenyl)propan-1-one as the starting material. Yellow solid; yield 60%. ^{1}H NMR (400 MHz, DMSO-d_6) δ 9.79 (s, 1H), 9.25 (s, 1H), 9.03 (d, J = 8.6 Hz, 1H), 8.21 (s, 1H), 8.19 (d, J = 7.9 Hz, 1H), 7.91 (d, J = 7.7 Hz, 1H), 7.83 (s, 1H), 7.78 (d, J = 8.6 Hz, 1H), 7.73 (t, J = 7.4 Hz, 2H), 7.62 (s, 1H), 7.35 (s, 1H), 7.33 (s, 1H), 7.30 (d, J = 7.8 Hz, 1H), 5.06−4.92 (m, 1H), 3.86 (s, 3H), 2.27 (s, 3H), 1.89 (qt, J = 13.7, 6.6 Hz, 2H), 0.94 (t, J = 7.2 Hz, 3H). ^{13}C NMR (126 MHz, DMSO-d_6) δ 164.86, 162.65, 156.98, 150.81, 141.91, 140.64, 136.08 (d, J = 4.4 Hz), 135.90, 133.86, 132.00, 130.88, 130.27, 130.06, 129.54 (d, J = 31.9 Hz), 128.47, 128.22 (d, J = 4.3 Hz), 128.03, 126.28, 125.52, 124.47 (d, J = 272.5 Hz), 124.33 (d, J = 4.0 Hz), 123.69, 121.07, 120.10, 55.34, 39.21, 29.41, 20.32, 11.85. HRMS m/z (ESI) found 545.2284 [M+H]$^+$, C$_{30}$H$_{28}$F$_3$N$_6$O$^+$ Calcd. for 545.2271, HPLC >99% pure.

4.2.41. N-(1-(3-(2-((1-Cyclopropyl-1H-pyrazol-4-yl)amino) quinazolin-6-yl)-4-methylphenyl)ethyl)-3-(trifluoromethyl) benzamide (43)

43 was prepared using the same method as **40** with 1-(3-bromo-4-methylphenyl)ethan-1-one as the starting material. Yellow solid; yield 52%. ^{1}H NMR (400 MHz, DMSO-d_6) δ 9.79 (s, 1H), 9.25 (s, 1H), 9.10 (d, J = 8.0 Hz, 1H), 8.23 (s, 2H), 8.19 (d, J = 7.9 Hz, 1H), 7.91 (d, J = 7.7 Hz, 1H), 7.83 (s, 1H), 7.77 (dd, J = 8.5, 1.9 Hz, 1H), 7.76−7.68 (m, 2H), 7.62 (s, 1H), 7.38−7.32 (m, 2H), 7.30 (d, J = 8.4 Hz, 1H), 5.31−5.16 (m, 1H), 3.74 (tt, J = 7.4, 3.9 Hz, 1H), 2.26 (s, 3H), 1.54 (d, J = 7.0 Hz, 3H), 1.06 (dt, J = 7.8, 3.8 Hz, 2H), 0.97 (dt, J = 6.6, 3.0 Hz, 2H). ^{13}C NMR (126 MHz, DMSO-d_6) δ 164.46, 162.68, 156.98, 150.77, 142.81,

140.66, 136.15, 136.09, 135.81, 133.83, 132.03, 130.92, 130.44, 130.05, 129.53 (d, J = 32.0 Hz), 128.23, 128.00, 125.78, 125.56, 124.49 (d, J = 272.5 Hz), 124.37, 124.34, 120.24, 120.13, 48.95, 33.14, 22.66, 20.29, 6.61. HRMS m/z (ESI) found 557.2277 [M+H]$^+$, $C_{31}H_{28}F_3N_6O^+$ Calcd. for 557.2271, HPLC >99% pure.

4.2.42. N-(1-(4-Cyclopropyl-3-(2-((1-cyclopropyl-1H-pyrazol-4-yl)amino)quinazolin-7-yl)phenyl)ethyl)-3-(trifluoromethyl)benzamide (44)

44 was prepared using the same method as **40** with 1-(3-bromo-4-cyclopropylphenyl)ethan-1-one as the starting material. Yellow solid; yield 59%. ^{1}H NMR (400 MHz, DMSO-d_6) δ 9.78 (s, 1H), 9.27 (s, 1H), 9.09 (d, J = 8.1 Hz, 1H), 8.27−8.21 (m, 2H), 8.19 (d, J = 8.0 Hz, 1H), 7.93−7.88 (m, 2H), 7.86 (dd, J = 8.6, 1.9 Hz, 1H), 7.72 (t, J = 7.9 Hz, 2H), 7.62 (s, 1H), 7.37−7.32 (m, 2H), 7.01 (d, J = 8.7 Hz, 1H), 5.22 (p, J = 7.5, 7.0 Hz, 1H), 3.74 (tt, J = 7.6, 4.1 Hz, 1H), 1.84 (ddt, J = 12.4, 9.0, 4.2 Hz, 1H), 1.53 (d, J = 7.0 Hz, 3H), 1.09−1.02 (m, 2H), 1.00−0.93 (m, 2H), 0.86−0.80 (m, 2H), 0.67 (q, J = 4.9 Hz, 2H). ^{13}C NMR (126 MHz, DMSO-d_6) δ 164.45, 162.70, 156.98, 150.77, 142.23, 141.12, 139.35, 136.44, 136.14, 135.79, 132.03, 130.43, 130.05, 129.53 (d, J = 31.8 Hz), 128.23, 127.89, 126.07, 125.46, 124.85, 124.47 (d, J = 272.3 Hz), 124.36, 124.33, 123.54, 120.21, 120.13, 48.92, 33.14, 22.59, 13.71, 9.82, 6.61. HRMS m/z (ESI) found 583.2438 [M+H]$^+$, $C_{33}H_{30}F_3N_7O^+$ Calcd. for 583.2428, HPLC >99% pure.

4.2.43. (R)-N-(1-(4-Cyclopropyl-3-(2-((1-cyclopropyl-1H-pyrazol-4-yl)amino)quinazolin-7-yl)phenyl)ethyl)-3-(trifluoromethyl)benzamide (45) and (S)-N-(1-(4-cyclopropyl-3-(2-((1-cyclopropyl-1H-pyrazol-4-yl)amino)quinazolin-7-yl)phenyl)ethyl)-3-(trifluoromethyl)benzamide (46)

N-(1-(3-Bromo-4-cyclopropylphenyl)ethyl)-3-(trifluoromethyl)benzamide (**m24**) were separated by chiral column with following condition: Superchiral S-AD (column size 0.46 cm × 15 cm, 5 μm), injection volume 1 μL, mobile phase Hexane/EtOH = 90/10 (v/v), flow rate 0.9 mL/min, wave length UV 220 nm and temperature 35 °C.

The retention time of *R* and *S* configuration were 3.715 and 4.649 min, respectively. These two intermediates were used to synthesize **45** and **46** by the same methods of **44**. The *R* and *S* chirality was determined according to the commercially available building blocks of **47** purchased later. **45**, yellow solid. ^{1}H NMR (400 MHz, chloroform-d) δ 9.06 (s, 1H), 8.20 (s, 1H), 8.03 (d, J = 2.0 Hz, 1H), 7.96 (d, J = 7.8 Hz, 1H), 7.86 (dd, J = 8.7, 2.0 Hz, 1H), 7.78−7.70 (m, 3H), 7.58 (s, 1H), 7.54 (t, J = 7.8 Hz, 1H), 7.35 (dd, J = 8.1, 2.0 Hz, 1H), 7.33−7.30 (m, 1H), 6.99 (d, J = 8.1 Hz, 1H), 6.58 (d, J = 7.7 Hz, 1H), 5.37 (p, J = 7.0 Hz, 1H), 3.67−3.57 (m, 1H), 1.90−1.79 (m, 1H), 1.65 (d, J = 6.9 Hz, 3H), 1.26 (s, 1H), 1.21−1.16 (m, 2H), 1.06−1.00 (m, 2H), 0.91−0.79 (m, 2H), 0.74−0.65 (m, 2H). ^{13}C NMR (151 MHz, chloroform-d) δ 165.21, 156.54, 141.47, 140.44, 140.12, 136.95, 136.69, 135.31, 130.36, 129.22, 128.14, 127.84, 127.68, 125.83, 124.89, 124.02, 122.36, 120.99, 120.20, 49.28, 32.98, 29.72, 21.72, 13.47, 9.74, 9.61, 6.54. HRMS m/z (ESI) found 583.2426 [M+H]$^+$, $C_{33}H_{30}F_3N_7O^+$ Calcd. for 583.2428, HPLC >98% pure. **46**, yellow solid. ^{1}H NMR (400 MHz, chloroform-d) δ 9.06 (s, 1H), 8.21 (s, 1H), 8.03 (s, 1H), 7.96 (d, J = 7.9 Hz, 1H), 7.86 (dd, J = 8.7, 2.0 Hz, 1H), 7.78−7.71 (m, 3H), 7.58 (s, 1H), 7.54 (t, J = 7.8 Hz, 1H), 7.43 (s, 1H), 7.38−7.29 (m, 2H), 6.99 (d, J = 8.0 Hz, 1H), 6.52 (d, J = 7.8 Hz, 1H), 5.37 (p, J = 7.1 Hz, 1H), 3.68−3.58 (m, 1H), 1.91−1.80 (m,

1H), 1.65 (d, J = 6.9 Hz, 3H), 1.23−1.14 (m, 2H), 1.10−0.97 (m, 2H), 0.91−0.79 (m, 2H), 0.74−0.66 (m, 2H). ^{13}C NMR (151 MHz, chloroform-d) δ 165.22, 162.01, 156.70, 150.89, 141.52, 140.43, 140.12, 136.83, 136.57, 135.32, 130.37, 129.21, 128.12, 127.83, 127.65, 125.83, 125.41, 124.86, 124.03, 124.01, 122.51, 120.93, 120.25, 49.29, 32.98, 21.72, 13.47, 9.75, 9.61, 6.54, 6.52. HRMS m/z (ESI) found 583.2438 [M+H]$^+$, $C_{33}H_{30}F_3N_7O^+$ Calcd. for 583.2428, HPLC >98% pure.

4.2.44. (S)-N-(1-(4-Cyclopropyl-3-(2-((1-(1-methylpiperidin-4-yl)-1H-pyrazol-4-yl)amino)quinazolin-7-yl)phenyl)ethyl)-3-(trifluoromethyl)benzamide (47)

47 was prepared using the same method as **40** with commercially available (S)-1-(3-bromo-4-cyclopropylphenyl)ethan-1-amine (ee>98%) starting material. Yellow solid; yield 48%. ^{1}H NMR (400 MHz, chloroform-d) δ 9.06 (s, 1H), 8.24 (s, 1H), 8.02 (s, 1H), 7.96 (d, J = 7.8 Hz, 1H), 7.86 (dd, J = 8.6, 2.0 Hz, 1H), 7.78−7.69 (m, 3H), 7.61 (s, 1H), 7.55 (t, J = 7.8 Hz, 1H), 7.38−7.28 (m, 3H), 7.00 (d, J = 8.1 Hz, 1H), 6.44 (d, J = 7.7 Hz, 1H), 5.37 (p, J = 7.0 Hz, 1H), 3.06−2.99 (m, 2H), 2.37 (s, 3H), 2.18 (q, J = 14.3, 12.4 Hz, 6H), 1.92−1.80 (m, 1H), 1.66 (d, J = 6.9 Hz, 3H), 0.90−0.81 (m, 2H), 0.74−0.66 (m, 2H). ^{13}C NMR (151 MHz, chloroform-d) δ 165.17, 161.98, 151.00, 140.00, 136.79, 136.51, 135.34, 130.32, 130.04, 129.25, 128.14, 127.81, 127.63, 125.80, 125.53, 124.88, 123.99, 123.97, 122.72, 120.28, 117.75, 54.73, 49.27, 46.05, 32.54, 21.69, 13.46, 9.73, 9.64. HRMS m/z (ESI) found 640.2998 [M+H]$^+$, $C_{36}H_{37}F_3N_7O^+$ Calcd. for 640.3006, HPLC >99% pure.

Author contributions

Qi Wang: Writing-original draft, visualization, investigation, methodology. Bixi Tang: Writing-original draft, visualization, investigation, methodology. Dandan Sun: Project administration, investigation. Ying Dong: Conceptualization, investigation. Yinchun Ji: Investigation. Huanyu Shi: Investigation. Liwei Zhou: Investigation. Yueyue Yang: Investigation. Menglan Luo: Investigation. Qian Tan: Investigation. Lin Chen: Investigation. Yue Dong: Investigation. Cong Li: Investigation. Rongrong Xie: Investigation. Yi Zang: Conceptualization, project administration, supervision, writing-review & editing Jingkang Shen: Conceptualization, project administration, supervision. Bing Xiong: Conceptualization, project administration, supervision, writing-review & editing. Jia Li: Conceptualization, project administration, supervision, Danqi Chen: Conceptualization, funding acquisition, project administration, supervision, writing-review & editing.

Conflicts of interest

The authors declare no conflicts of interest.

Appendix A. Supporting information

Supporting information to this article can be found online at https://doi.org/10.1016/j.apsb.2021.11.012.

References

1. Rosas IO, Dellaripa PF, Lederer DJ, Khanna D, Young LR, Martinez FJ. Interstitial lung disease: NHLBI workshop on the primary prevention of chronic lung diseases. *Ann Am Thorac Soc* 2014; **11**(Suppl 3):S169−77.
2. Diamantopoulos A, Wright E, Vlahopoulou K, Cornic L, Schoof N, Maher TM. The burden of illness of idiopathic pulmonary fibrosis: a comprehensive evidence review. *Pharmacoeconomics* 2018;**36**: 779−807.
3. Fu HL, Valiathan RR, Arkwright R, Sohail A, Mihai C, Kumarasiri M, et al. Discoidin domain receptors: unique receptor tyrosine kinases in collagen-mediated signaling. *J Bio Chem* 2013;**288**:7430−7.
4. Leitinger B. Transmembrane collagen receptors. *Annu Rev Cell Dev Biol* 2011;**27**:265−90.
5. Leitinger B. Discoidin domain receptor functions in physiological and pathological conditions. *Int Rev Cell Mol Biol* 2014;**310**:39−87.
6. Borza CM, Pozzi A. Discoidin domain receptors in disease. *Matrix Biol* 2014;**34**:185−92.
7. Kothiwale S, Borza CM, Lowe Jr EW, Pozzi A, Meiler J. Discoidin domain receptor 1 (DDR1) kinase as target for structure-based drug discovery. *Drug Discov Today* 2015;**20**:255−61.
8. Vogel W, Gish GD, Alves F, Pawson T. The discoidin domain receptor tyrosine kinases are activated by collagen. *Mol Cell* 1997;**1**:13−23.
9. Bian H, Nie X, Bu X, Tian F, Yao L, Chen J, et al. The pronounced high expression of discoidin domain receptor 2 in human interstitial lung diseases. *ERJ Open Res* 2018;**4**:00138-2016.
10. Guyard A, Danel C, Theou-Anton N, Debray MP, Gibault L, Mordant P, et al. Morphologic and molecular study of lung cancers associated with idiopathic pulmonary fibrosis and other pulmonary fibroses. *Respir Res* 2017;**18**:120.
11. Zhao H, Bian H, Bu X, Zhang S, Zhang P, Yu J, et al. Targeting of discoidin domain receptor 2 (DDR2) prevents myofibroblast activation and neovessel formation during pulmonary fibrosis. *Mol Ther* 2016; **24**:1734−44.
12. Ruiz PA, Jarai G. Collagen I induces discoidin domain receptor (DDR) 1 expression through DDR2 and a JAK2-ERK1/2-mediated mechanism in primary human lung fibroblasts. *J Biol Chem* 2011;**286**: 12912−23.
13. Li Y, Lu X, Ren X, Ding K. Small molecule discoidin domain receptor kinase inhibitors and potential medical applications. *J Med Chem* 2015;**58**:3287−301.
14. Murray CW, Berdini V, Buck IM, Carr ME, Cleasby A, Coyle JE, et al. Fragment-based discovery of potent and selective DDR1/2 inhibitors. *ACS Med Chem Lett* 2015;**6**:798−803.
15. Jeffries DE, Borza CM, Blobaum AL, Pozzi A, Lindsley CW. Discovery of vu6015929: a selective discoidin domain receptor 1/2 (DDR1/2) inhibitor to explore the role of DDR1 in antifibrotic therapy. *ACS Med Chem Lett* 2020;**11**:29−33.
16. Gao M, Duan L, Luo J, Zhang L, Lu X, Zhang Y, et al. Discovery and optimization of 3-(2-(pyrazolo[1,5-*a*]pyrimidin-6-yl)ethynyl) benzamides as novel selective and orally bioavailable discoidin domain receptor 1 (DDR1) inhibitors. *J Med Chem* 2013;**56**: 3281−95.
17. Wang Z, Bian H, Bartual SG, Du W, Luo J, Zhao H, et al. Structure-based design of tetrahydroisoquinoline-7-carboxamides as selective discoidin domain receptor 1 (DDR1) inhibitors. *J Med Chem* 2016;**59**:5911−6.
18. Richter H, Satz AL, Bedoucha M, Buettelmann B, Petersen AC, Harmeier A, et al. DNA-encoded library-derived DDR1 inhibitor prevents fibrosis and renal function loss in a genetic mouse model of alport syndrome. *ACS Chem Biol* 2019;**14**:37−49.
19. Wang Q, Dai Y, Ji Y, Shi H, Guo Z, Chen D, et al. Discovery and optimization of a series of 3-substituted indazole derivatives as multi-target kinase inhibitors for the treatment of lung squamous cell carcinoma. *Eur J Med Chem* 2019;**163**:671−89.
20. Nanthakumar CB, Hatley RJ, Lemma S, Gauldie J, Marshall RP, Macdonald SJ. Dissecting fibrosis: therapeutic insights from the small-molecule toolbox. *Nat Rev Drug Discov* 2015;**14**:693−720.
21. Hameed A, Al-Rashida M, Uroos M, Ali SA, Arshia Ishtiaq M, Khan KM. Quinazoline and quinazolinone as important medicinal scaffolds: a comparative patent review (2011−2016). *Expert Opin Ther Pat* 2018;**28**:281−97.
22. Hilberg F, Tontsch-Grunt U, Baum A, Le AT, Doebele RC, Lieb S, et al. Triple angiokinase inhibitor nintedanib directly inhibits tumor cell growth and induces tumor shrinkage *via* blocking oncogenic receptor tyrosine kinasess. *J Pharmacol Exp Therapeut* 2018;**364**: 494−503.
23. Avivi-Green C, Singal M, Vogel WF. Discoidin domain receptor 1-deficient mice are resistant to bleomycin-induced lung fibrosis. *Am J Respir Crit Care Med* 2006;**174**:420−7.